GEOLOGICAL SURVEY OF CANADA
OPEN FILE 7333

Permafrost modelling in northern Great Slave region Northwest Territories, Phase 1: Climate data evaluation and 1-d sensitivity analysis

D. W. Riseborough, S.A. Wolfe and C. Duchesne

2013

Natural Resources Canada | Ressources naturelles Canada

Canada

GEOLOGICAL SURVEY OF CANADA
OPEN FILE 7333

Permafrost modelling in northern Great Slave region Northwest Territories, Phase 1: Climate data evaluation and 1-d sensitivity analysis

D. W. Riseborough, S.A. Wolfe and C. Duchesne

2013

doi:10.4095/292366
This publication is available for free download through GEOSCAN (http://geoscan.ess.nrcan.gc.ca/).

Recommended citation
Riseborough, D.W., Wolfe, S.A., and Duchesne, C., 2013. Permafrost modelling in northern Slave region Northwest Territories, Phase 1: Climate data evaluation and 1-d sensitivity analysis; Geological Survey of Canada, Open File 7333, 50p. doi:10.4095/292366

Publications in this series have not been edited; they are released as submitted by the author.

ABSTRACT

Climate variables were examined to evaluate their use in permafrost models, using data for Yellowknife Northwest Territories, Canada as an example. Results suggest that conversion of the annual temperature cycle to a sine wave is an acceptable approximation, as long as the wave retains the correct values for the annual freezing and thawing degree-day totals. Changes in snow depth can be approximated by a parabolic accumulation function. The delay of snow cover initiation with respect to the start of the freezing season, the snow accumulation function, and snow density are all critical, whereas end-of-season snowpack evolution is of secondary importance.

Modelling results show that *any* difference in substrate materials produces a change in the mean annual temperature at the top-of-perennially frozen/unfrozen ground (TTOP) and annual maximum freezing/thawing layer thickness (AFTT). The greatest differences in TTOP were produced by changes in the thickness and degree of saturation of the surface organic layer. Intermediate differences were due to differences in substrate materials within and immediately below the annual freezing/thawing layer itself, and the smallest differences were due to variations in the substrate well below the thickness of the annual freezing/thawing layer. These results suggest that knowledge or consideration of the thickness and moisture content of organic soil veneers will be vital to permafrost mapping in this environment.

TABLE OF CONTENTS

LIST OF FIGURES

Figure 13. Using data for Yellowknife 1955-2005: a) Relationship between annual maximum snow depth and ablation-period TDD derived from daily mean temperature; b) Relationship between annual maximum snow depth and ablation-period TDD derived from daily maximum & minimum temperature; c) Relationship between snow depth at start of ablation and ablation-period TDD derived from daily mean temperature; d) Relationship between snow depth at start of ablation and ablation-period TDD derived from daily maximum & minimum temperature; e) Distribution of calculated M_f from data in (a), assuming a snow density of 212. kg m-2 (mean for April 15 in Figure 7) derived for seasonal maximum and freezing-season end.

Figure 14. Temperature dependent a) thermal conductivity ($Wm^{-1}K^{-1}$) and b) unfrozen volumetric water content (fraction) for wet clay soil used in simulation modelling.

Figure 15. Stratigraphic profiles of representative terrain types used in simulation modelling.

Figure 16. Stratigraphic profiles of special terrain types used in simulation modelling.

Figure 17. Results for representative terrain types, using 1955-2006 Yellowknife climate statistics with organic layers (saturated and unsaturated) 20 cm thick Square symbols indicate 51-year mean. a) mean annual temperature at the top-of-perennially frozen/unfrozen ground (TTOP). b) Simulated maximum annual freezing/thawing layer thickness (AFTT) values. Boxes and whiskers show maximum, upper quartile, median, lower quartile and minimum values for 1955-2006 for each thickness.

Figure 18. Simulated mean annual temperature at the top-of-perennially frozen/unfrozen ground (TTOP) and annual maximum annual freezing/thawing layer thickness (AFTT) values for sand and clay substrates of different configurations, all with 20 cm organic layer (saturated and unsaturated), using 1955-2006 Yellowknife climate statistics. Boxes and whiskers show maximum, upper quartile, median, lower quartile and minimum values for 1955-2006 for each thickness.

Figure 19. Effect of varying organic layer thickness on simulated mean annual temperature at the top-of-perennially frozen/unfrozen ground (TTOP) and maximum annual freezing/thawing layer thickness (AFTT) values for wet clay substrate terrain, using 1955-2006 Yellowknife climate statistics. Boxes and whiskers show maximum, upper quartile, median, lower quartile and minimum values for 1955-2006 for each thickness.

Figure 20. Effect of varying organic layer thickness on simulated mean annual temperature at the top-of-perennially frozen/unfrozen ground (TTOP) and maximum annual freezing/thawing layer thickness (AFTT) values for sand substrate terrain, using 1955-2006 Yellowknife climate statistics.

Figure 21. Effect of varying organic layer thickness on simulated mean annual temperature at the top-of-perennially frozen/unfrozen ground (TTOP) and maximum annual freezing/thawing layer thickness (AFTT) values for bedrock substrate terrain, using 1955-2006 Yellowknife climate statistics. Boxes and whiskers show maximum, upper quartile, median, lower quartile and minimum values for 1955-2006 for each thickness.

LIST OF TABLES

Permafrost modelling in northern Great Slave region Northwest Territories, Phase 1: Climate data evaluation and 1-d sensitivity analysis

INTRODUCTION

Permafrost is an important component of the landscape within the extensive discontinuous permafrost zone of the Great Slave region (Figure 1). Although the state and distribution of permafrost in the area have been described through a few reconnaissance studies (e.g. Karunaratne *et al*. 2008, Brown 1973), field data on ground temperatures and stratigraphy remain limited. This study presents the first steps in an evaluation of current and future permafrost conditions in the Slave region through permafrost modelling.

The objective of this study is to explore the basic climate-permafrost relationships in the northern Great Slave region (NGSR) using spatial permafrost models, and to examine the thermal behaviour of the ground at key landscape transitions that contribute to increased infrastructure maintenance and enhanced sensitivity to permafrost degradation. In this preliminary phase, the combined role of climate (air temperature and snow fall / snow cover) and substrate materials (organic and mineral soil, and bedrock) in determining the range of ground thermal regimes of the NGSR is evaluated using one dimensional thermal simulation modelling.

The first part of this report summarises the Yellowknife climate record, and examines some of the simplifying approaches that can be applied to climate data for model input. Numerical permafrost simulation models are used to estimate the thermal state of the ground, including predicted future changes. A critical process in model building is to balance scientifically realistic complexity with practically realistic simplicity (Ferguson 1999). Model outputs are influenced by model inputs, so it is important to consider the effect of simplifying assumptions on the accuracy of simulation results.

The second part of this report applies the derived climate parameters to a range of typical Great Slave region environments, as defined by their substrate materials. The NGSR is dominated by a limited number of terrain types: bedrock outcrop, peatland (peat typically 1-2 m thick), taiga forests (aspen-birch or spruce) over shallow sand or clay, and small lakes and ponds.

Regional Setting

The region between Yellowknife and Behchoko, along the north shore of Great Slave Lake, resides within the Great Slave Lowland High Boreal Ecoregion (Figure 2). Bedrock, wet fens and saturated bogs are typically devoid of permafrost in this area, whereas spruce and deciduous forests and peatlands typically contain permafrost, though at relatively warm temperatures (Wolfe, 1998; Gaandarse, 2011). Thus, the presence of permafrost in this region is highly variable, with abrupt transitions from frozen to unfrozen ground usually occurring over short distances. Whereas thick ice lenses and possibly massive ground ice can be found in the area (Aspler, 1978; EBA, 1995), thinner (1 to 20 mm thick) ice lenses are more common, primarily in clays of glaciolacustrine origin. These clays represent the dominant surficial unit in the region, and were deposited by Glacial Lake McConnell between about 10 and 8.5 ka BP (Lemmen *et al*., 1994; Smith, 1994).

The only all-weather ground-based transportation access to and from Yellowknife is via Highway 3, which extends across the discontinuous permafrost zone and the high boreal ecoregion (Figures

1 and 2). During the mid-1960s, the first all-weather road access was constructed along the route between Yellowknife and Behchoko (formerly Rae-Edzo). Between 1999 and 2006, the highway route between Yellowknife and Behchoko was upgraded with major realignments for the purpose of straightening the road and maximizing the portion of the road that is on bedrock (EBA, 1995).

Before and after construction, several engineering studies were conducted (EBA, 1995, 1998, 2003a and 2003b), which provide background to the pre-existing and as-built geotechnical and geothermal conditions. These reports indicate that where permafrost is present it is generally warm (-1°C or warmer) and contains excess ground ice (EBA, 2003b) within the fine-grained soils. This permafrost is very sensitive to factors that affect natural surface heat transfer conditions such as removal of vegetation and alteration of snowdrift patterns, and is also sensitive to climatic variations (EBA, 2003b).

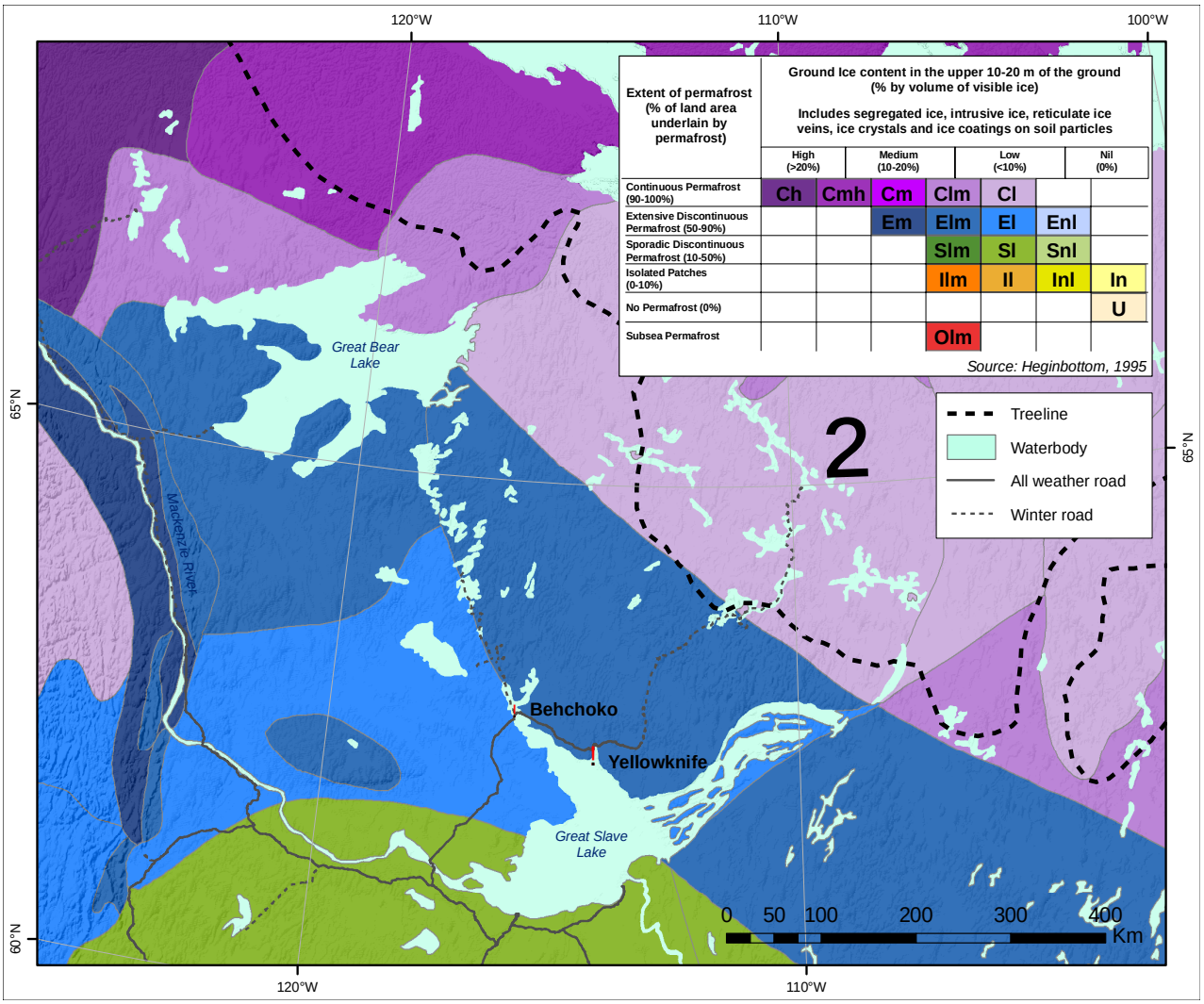

Figure 1. Permafrost and ground ice in western Canada. The Yellowknife region resides within the extensive discontinuous permafrost zone with a low-to-medium ground ice content (after Heginbottom et al., 1995).

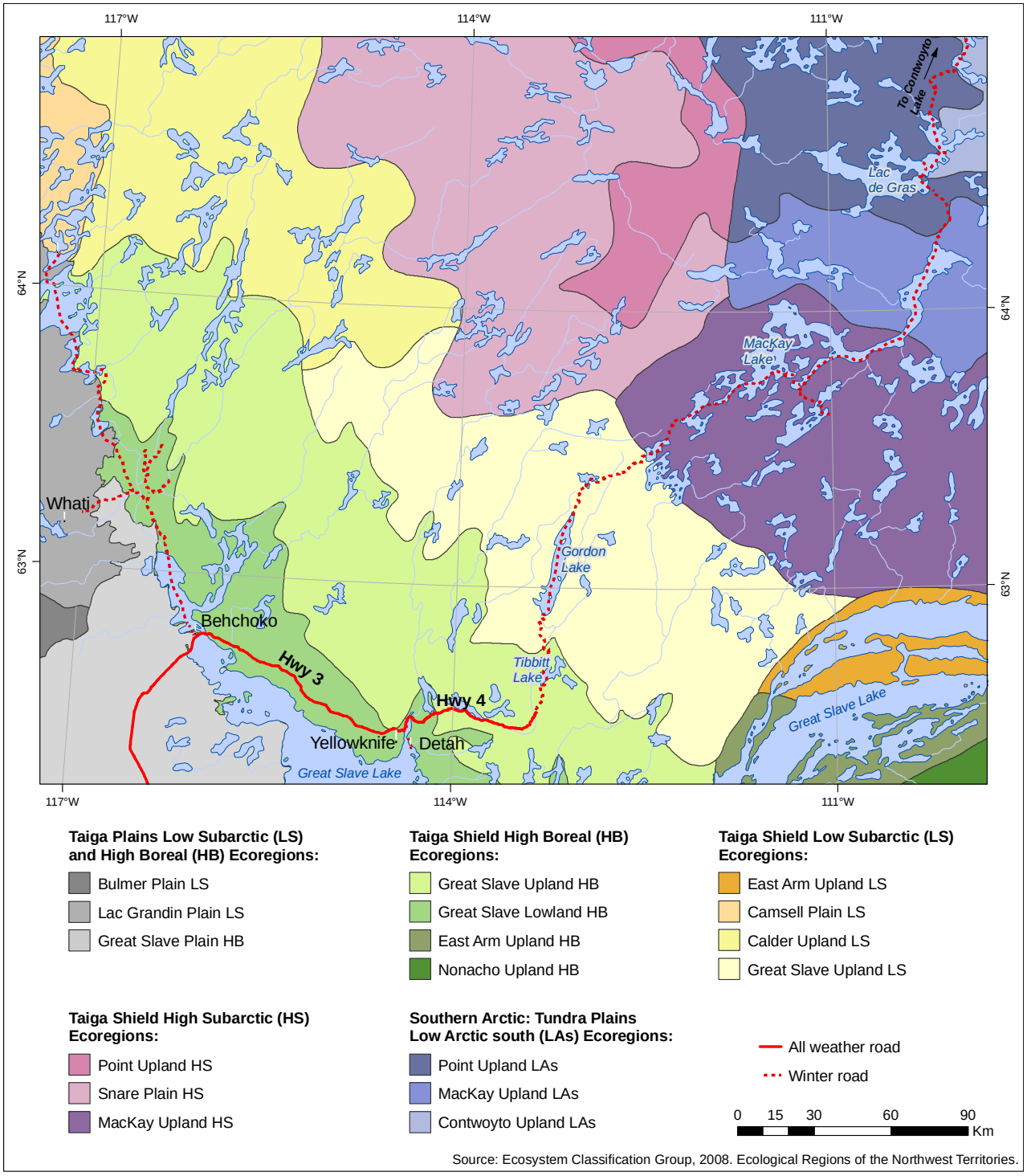

Figure 2. Taiga Shield Ecoregions, depicting the Great Slave Lowland High Boreal Ecoregion. (Ecosystem Classification Group, 2008).

Terminology in this document

Permafrost is defined as earth material ("ground") that remains below zero degrees Celsius (0°C) over at least two consecutive years (van Everdingen, 1998). The active layer is the ground above permafrost that undergoes seasonal freezing and thawing (Burn 1998). The term active layer has been reserved for such a layer above permafrost only: where permafrost is not present, the term "seasonally frozen surface layer" is used (van Everdingen 1998). The bottom of the active layer is usually the top of permafrost, except in transient conditions where inter-annual variations or ongoing thaw leads to the persistence of unfrozen ground over the winter. Where the discussion is unambiguously about permafrost or non-permafrost, "active layer" and "seasonally frozen layer" are used in this way. Where the ground thermal state below the surface layer is unclear (such as when discussing model results), "seasonally frozen/thawed layer" is used.

When introduced, the model acronym TTOP initially stood for "Temperature at the Top Of Permafrost" (Smith and Riseborough 1996). The acronym is used here although it is recognized that the model is also applied where there is no permafrost. TTOP defines the mean annual "Temperature at Top Of Perennially frozen/unfrozen ground".

When permafrost is degrading, or in a year following the development of an exceptionally deep active layer, a layer of soil may remain unfrozen through the winter (referred to as a *talik*). In these cases the term TTOP is used, but refers to the mean annual temperature at the base of the active layer; the mean annual temperature at the top of permafrost (i.e. at the base of the *talik*) in these cases will be very close to 0°C.

Acronyms used in this document have the following definitions:

AFTT: annual maximum freezing/thawing layer thickness

ALT: annual maximum active layer thickness

FDD: freezing degree days

FDD_{Ann}: annual total freezing degree days

MAAT: mean annual air temperature

MSC: Meteorological Service of Canada

NGSR: northern Great Slave region

OLT: organic layer thickness

SWE: snow water equivalent

TDD: thawing degree-days

TDD_{Ann}: annual total thawing degree-days

TTOP: mean annual temperature at top of perennially frozen/unfrozen ground

WMO: World Meteorological Organization

MAGT: mean annual ground temperature

CLIMATE DATA ANALYSIS

The Yellowknife area has a continental climate, with mean annual air temperature (MAAT) of -4.6°C and mean daily temperatures ranging from 17°C in July to -26°C in January (Environment Canada, 2012). Mean total precipitation is 281 mm, with about 58% falling as rain. The average annual recorded maximum depth of snow on the ground is 0.46 m, with a range from 0.25 m to 0.71 m within the 1971-2000 normal period. Mean annual air temperatures also indicate a warming trend of about 0.3°C per decade since the 1940s (Riseborough *et al*., 2012; Hoeve *et al*., 2004), and an accelerated trend of about 0.6°C per decade since 1970 (Hoeve et. al, 2004).

In this analysis the goal is to characterize ground thermal behaviour at an annual time scale, rather than to predict the actual day-to-day seasonal progression of the ground thermal regime: for example, results for maximum annual freezing/thawing layer thickness (AFTT) are more important than the timing of the freeze/thaw front position over the season. As such, trends and inter-annual variation in freezing and thawing degree-days should be represented in model input, but daily or synoptic-scale variations are not required. Conceptual descriptions of permafrost-climate interactions (Smith and Riseborough, 2002), model-based sensitivity analyses (Goodrich, 1982, Ling and Zhang, 2006, 2007) and field studies (Smith *et al*., 2009) suggest that the key climate variables for model input are:

- Mean annual air temperature (MAAT)
- Annual total freezing degree-days (FDD_{Ann})
- Annual total thawing degree-days (TDD_{Ann})
- MAAT, FDD_{Ann} and TDD_{Ann} trends (°C and C°-days/decade)
- Inter-annual variability
- Snow cover initiation
- Snow density
- Seasonal pattern of snow accumulation
- Snow ablation

Specification of these parameters is discussed in the following sections.

Climate data processing

Basic multi-year average annual statistics derived from daily data are shown in Table 1, including mean annual temperature, annual total freezing and thawing degree-days, annual mean and maximum depth of snow on-the-ground, and seasonal timing of the maximum snow depth (note that the annual mean snow depth is the average only for the days in which snow depth is greater that a trace). Statistics on some additional parameters important to the specification of snow cover in modelling the ground thermal regime were also derived from the daily data, including thawing degree-days during the snow ablation period, and snow-free freezing days and freezing degree-days at the beginning of the freezing season. These parameters were computed using daily climate station data from Environment Canada (online at http://climate.weatheroffice.gc.ca/climateData/), comprised of the daily mean temperatures, and daily depth of snow-on-ground for the years 1955-2006 for the Yellowknife A weather station (WMO Identifier 71936). The year 1955 was the first for which daily depth of snow-on-ground were available, and 2006 was the latest year for which snow-on-ground depth was available at the time that the analysis was performed. Note that daily mean temperatures in the climate record are calculated as the average of the daily maximum and minimum values. Methods for computing parameter values are given below.

Table 1. Climate statistics for thermal permafrost modelling based on Yellowknife Airport weather station data 1955-2006. Regression statistics that are significantly different from random ($p < 0.05$) are shown in bold text.

Parameter	Mean	Median	Minimum	Maximum	St. Dev.	Trend (per decade)	Trend R^2	Trend p	N
Mean annual air temperature (°C)	-4.8	-5.0	-7.5	-1.2	1.41	+**0.49**	**0.267**	**0.000**	51
Annual freezing degree-days (C °-days)	3525	3660.7	2330.8	4387	440	**-151**	**0.270**	**0.000**	52
Annual thawing degree-days (C °-days)	1790	1792.1	1485.9	2182.8	144	**+30**	**0.099**	**0.023**	52
Mean snow depth (cm)	26.9	25.1	10.3	47.1	8.57	+0.8	0.021	0.324	49
Maximum snow depth (cm)	45.8	45.0	20.0	81.0	13.1	+0.1	0.000	0.940	49
Date of maximum snow depth (latest)	14-Mar	17-Mar	14-Jan	24-Apr	21.9	-1.5 days	0.011	0.475	49
First day of persistent snow (date)	26-Oct	28-Oct	26-Sep	23-Nov	10.9	-0.9 days	0.017	0.368	51
First Spring day without snow (date)	30-Apr	01-May	01-Apr	21-May	9.8	**-2.1 days**	**0.107**	**0.022**	49
Freezing continuous from (date)	25-Oct	26-Oct	07-Oct	09-Nov	8.7	-0.9 days	0.021	0.629	49
Freezing continuous until (date)	11-Apr	11-Apr	27-Feb	03-May	11.7	**-2.5 days**	**0.098**	**0.031**	51
Autumn snow-free freezing days (C °-days)	8.9	9.5	0.0	25	5.8	**-1.3**	**0.111**	**0.018**	50
Autumn snow-free freezing degree-days (C °-days)	41.9	29.4	0.0	144.1	34.3	**-7.2**	**0.140**	**0.008**	48
Spring ablation thawing degree-days (C °-days)	19.6	15.4	1.3	91.3	16.9	+1.2	0.010	0.515	46

Missing values

To generate annual statistics using the daily mean air temperature and depth of snow-on-ground for the years 1955-2006, all data gaps but one (the longest gap in the depth-of-snow-on-ground data) were filled with values estimated by linear interpolation between the values on either side of the gap. The data were assembled (in a spreadsheet) as a nearly-continuous 51 year record. From 1955 to 1991, the daily air temperature record contains no gaps whereas the daily depth-of-snow-on-ground has a single 2-day gap. Between 1992 and 2006 the record contains numerous short gaps: the air temperature record includes four years with at least one gap during this period, with missing data for 59 days in 1992, and no other gap longer than 4 days. For the depth-of-snow-on-ground data, the record is somewhat more complicated due to the number of years with missing values (all presumed zero) for the extended period with no snow cover, and because the snow cover season is spread across two calendar years. There are 9 years with missing data, 3 of which have missing data only in the period for which it is reasonable to assume that all missing data values are zero. Of the remaining 6 years with missing data, 2 have short blocks of missing data (many periods of up to 4 days) while the missing data for the other years comprise two extended periods spanning across calendar years. Snow depths were estimated by linear interpolation for the shorter data gaps. No attempt was made to interpolate values for longer data gaps, resulting in missing values for those annual parameters that aggregate the full season's data.

Dates for key winter events

Annual dates for key winter events (Figure 5) were determined from the daily temperature and snow depth data using the following criteria:

- The date for the start of **continuous freezing** was taken as the day following the last day with a mean temperature greater than 0°C, in the period between July 1 and December 31. Between 1955 and 2006, this date ranged from October 7 to November 9.
- The date for the **start of continuous snow cover** was taken as the day following the last day with a snow depth of 0 cm, in the period between July 1 and December 31. Between 1955 and 2006, this date ranged from September 26 to November 23.
- The date of **maximum snow depth** was taken as the *latest* date recording the maximum snow depth for that winter, in the period between July 1 and June 30 of the following year. Between 1955 and 2006, this date ranged from January 14 to April 24.
- The date for the **beginning of the thaw season** was taken as the first day when the daily mean air temperature is greater than 0°C in the period between January 1 and July 31. Between 1955 and 2006, this date ranged from February 27 (an outlier in the distribution – the second-earliest date is March 22) to May 3.
- The date for the **end of continuous snow cover** was taken as the first day with a snow depth of 0 cm, in the period between January 1 and July 31. Between 1955 and 2006, this date ranged from April 1 to May 21.

Trends

All of the climate variables based solely on temperature (Figure 3 a-c: mean annual air temperature, annual freezing and thawing degree-days) show significant trends consistent with a warmer climate, whereas trends in variables based solely on snow cover (Figure 3 d: mean and maximum snow depth) are not significantly different from random. Of the parameters describing

the interaction of the air temperature and the snow cover, the parameters relating to freezing without snow cover (Figure 4 a-b: autumn snow-free freezing days and degree-days) show a significant declining trend, while the spring ablation thawing degree-days (Figure 4 c) do not. Although the timing of all of the key winter events identified show a trend to earlier dates, only the commencement of thawing and the completion of snowmelt show a large and significant shift (12.5 days and 10.5 days earlier) over 50 years.

Snow-free freezing days and snow-free freezing degree-days

Snow-free freezing days (Figure 4a) are days leading to the commencement of the snow season that have a daily mean air temperature below 0°C but no snow cover (i.e. depth of snow on ground = 0); the annual total of snow-free freezing days is used as an input to the thermal model. Annual totals were calculated as the number of days from July 1 to December 31 with mean daily air temperatures below 0°C and depth of snow on ground = 0. The Yellowknife record indicates no snow-free freezing days before September 21 or later than November 23 in any year. Snow-free freezing degree-days (Figure 4b) are calculated as the degree-day total for the snow-free freezing days. Note that the total does not include freezing degree-days for any days with a mean daily temperature above 0°C, even when the daily minimum temperature is below 0°C.

Ablation degree-days

Ablation degree-days (Figure 4c) are the thawing degree-days associated with the end of the snow cover, and are used to calculate the melt-factor used to drive the ablation process in the thermal model (see *Snow ablation* section below). They were calculated as the sum of daily air temperatures above 0°C for all days between January 1 and the date that the depth of snow on ground first equals 0. Except for a single thawing day on February 27 1985, no thawing degree-days were recorded before March 22. Note that the total does not include degree-days for the ablation of late-falling new snow once the depth of snow reaches zero, and does not include degree-days for any days with a mean daily temperature below 0°C, even when the daily maximum temperature is above 0°C.

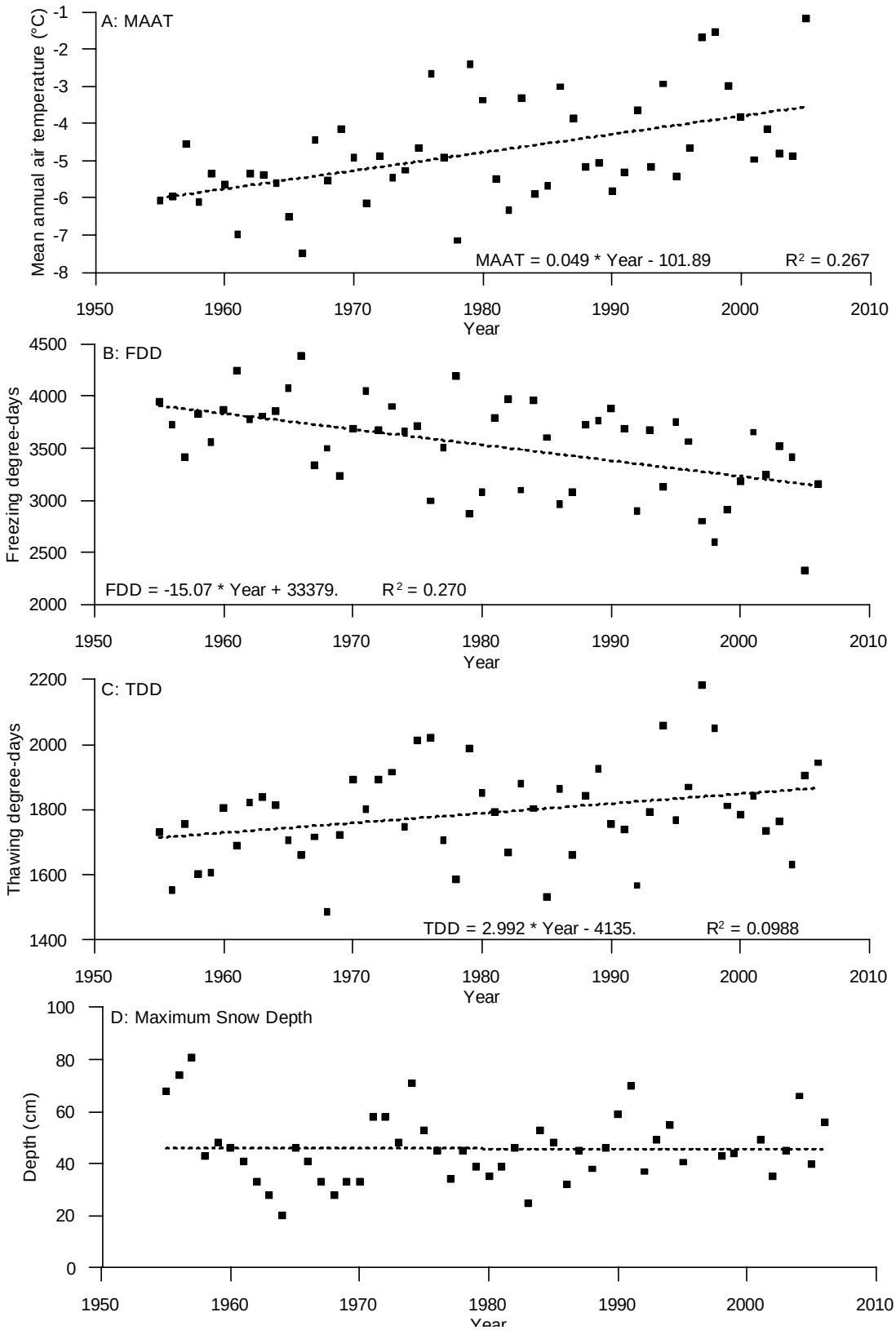

Figure 3. Basic climate statistics for Yellowknife, 1955-2006. Note that statistics are based on hydrological years (July 1 – June 30), with points assigned to the July-December year. Regression statistics are shown for statistically significant relationships only.

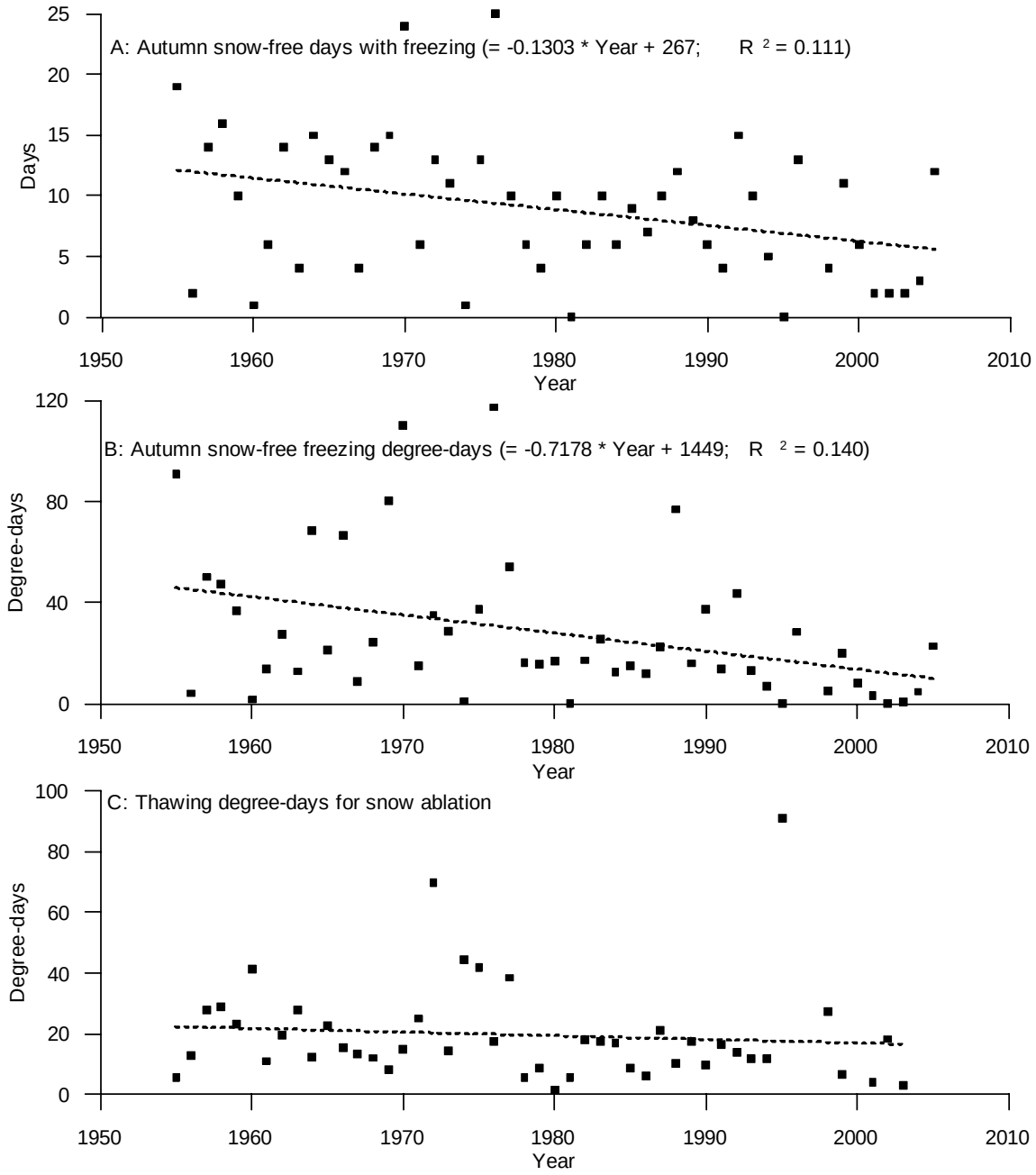

Figure 4. Climate statistics for Yellowknife, 1955-2006. Note that statistics are based on hydrological years (July 1 – June 30), with points assigned to the July-December year. Regression results are shown for statistically significant relationships only.

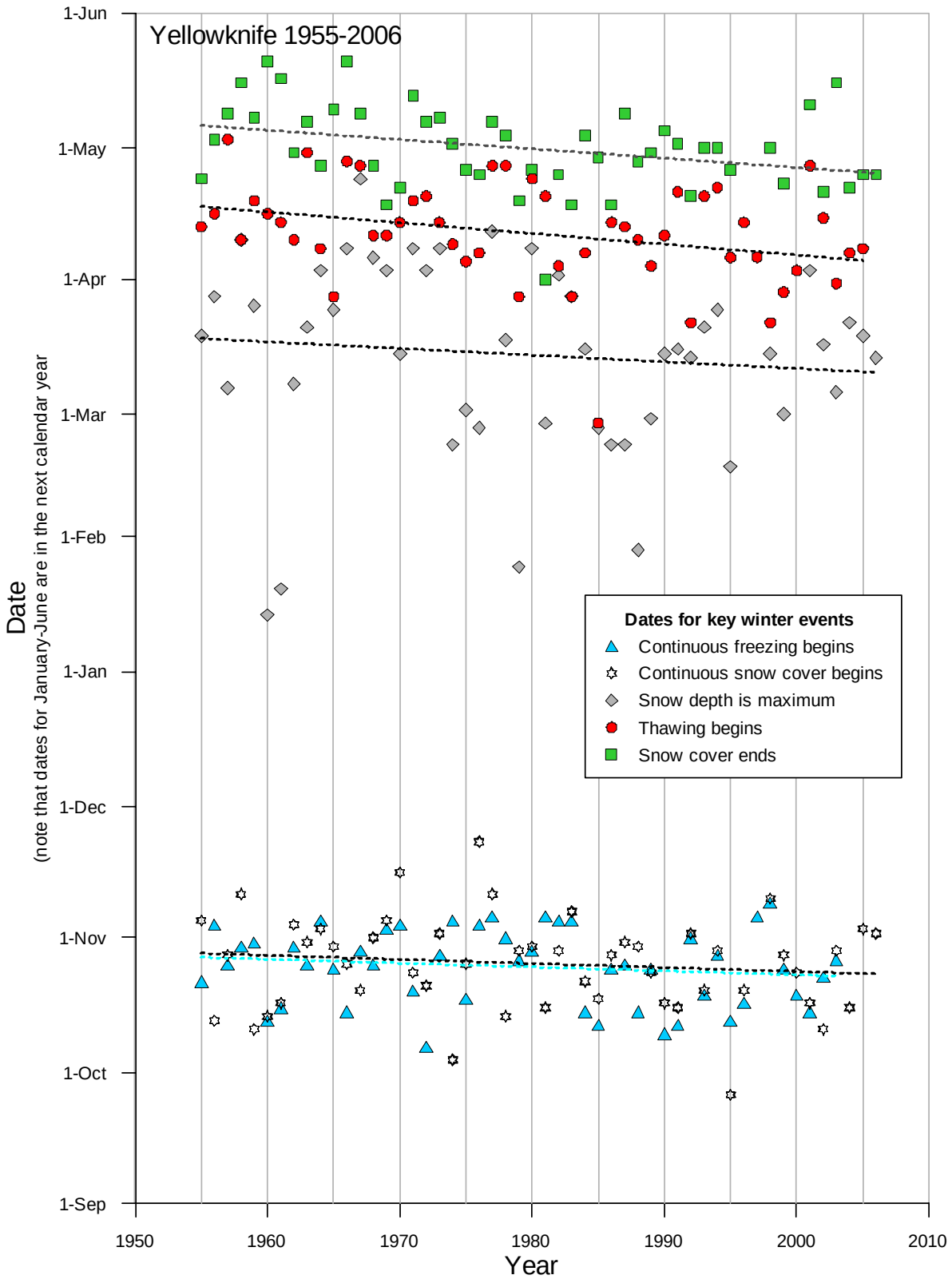

Figure 5. Dates for key thermal events of the freezing/snow cover season, Yellowknife 1955-2006. Note that time is continuous on the Y-axis, so that points in January and later are in the next calendar year.

Table 2. Multi-year average snow density through winter in the NGSR, from data in Meteorological Service of Canada (2000). Data for grid point nearest Yellowknife are shown in **bold**.

Lat	*Long*	*15-Nov*	*01-Dec*	*15-Dec*	*01-Jan*	*15-Jan*	*01-Feb*	*15-Feb*	*01-Mar*	*15-Mar*	*01-Apr*	*15-Apr*	*01-May*	*15-May*
62	-117	165.0	153.3	162.4	171.5	176.4	178.1	188.8	196.0	193.1	222.9	232.0	273.8	339.3
62	-116	167.3	161.2	168.6	177.2	182.6	186.4	197.2	204.1	201.3	228.5	239.0	274.7	330.6
62	-115	171.8	167.1	173.0	182.7	186.1	192.2	202.0	209.9	211.9	231.5	253.4	280.1	324.4
62	**-114**	**174.1**	**157.2**	**175.3**	**169.9**	**189.1**	**178.6**	**205.5**	**194.9**	**218.9**	**211.6**	**258.1**	**287.3**	**308.3**
62	-113	173.1	139.7	174.5	146.4	191.6	154.0	208.2	168.9	225.5	184.3	230.5	288.7	296.7
62	-112	170.4	143.4	173.7	152.6	194.0	155.0	207.6	167.7	227.9	183.1	211.3	288.0	298.1
62	-111	169.1	153.1	174.5	169.3	196.6	178.4	207.6	194.9	230.1	198.6	201.7	289.3	301.7
62	-110	168.5	162.6	176.7	185.1	198.5	196.1	208.2	214.3	231.4	217.5	197.0	290.5	306.5
62	-109	168.6	167.7	178.8	195.3	199.8	205.1	209.3	223.0	232.9	234.8	202.4	291.5	312.6
63	-117	171.5	159.5	171.5	163.2	185.9	169.5	200.9	187.9	224.9	263.5	209.8	296.1	341.1
63	-116	175.4	166.8	178.6	166.5	197.7	175.4	213.0	190.0	231.9	247.7	217.9	303.6	332.2
63	-115	178.3	169.1	183.2	174.0	200.2	182.2	218.7	193.8	237.1	237.3	232.0	306.6	324.7
63	-114	179.0	155.7	184.1	164.7	198.3	174.1	216.3	184.4	233.7	212.0	238.3	301.4	309.4
63	-113	176.0	139.7	182.3	147.0	199.0	153.9	214.7	167.6	234.5	182.5	230.9	298.0	296.0
63	-112	173.0	145.1	181.4	155.1	201.0	160.2	214.3	175.1	236.3	192.5	219.2	294.6	295.9
63	-111	171.9	157.3	181.1	173.8	203.1	183.8	214.5	203.4	238.0	222.8	222.7	293.3	299.3
63	-110	171.6	168.0	181.5	189.5	204.9	197.1	214.3	217.1	239.4	243.3	240.4	292.5	302.9
63	-109	171.9	174.4	182.3	200.8	206.5	207.7	214.2	226.0	240.4	256.2	260.8	292.0	308.0
64	-117	171.4	159.0	177.9	148.2	188.8	154.6	204.0	169.4	228.5	243.6	191.5	303.6	338.0
64	-116	173.3	160.3	182.9	152.2	197.7	160.3	213.9	167.5	239.7	232.8	183.3	305.6	327.4
64	-115	175.0	159.2	185.4	155.5	199.8	163.5	216.8	164.0	233.6	221.2	186.2	303.6	317.2
64	-114	175.7	155.5	184.8	156.5	198.6	165.8	214.6	170.1	232.4	208.9	210.9	298.6	310.4
64	-113	175.3	153.0	183.8	156.2	199.6	161.3	214.0	184.3	234.4	201.3	220.9	296.6	305.2
64	-112	174.9	153.5	183.1	162.1	201.2	167.5	214.0	195.1	236.2	208.8	225.7	295.0	305.9
64	-111	175.4	157.2	182.3	176.9	202.2	188.7	213.6	208.4	237.2	226.7	231.2	294.6	307.4
64	-110	176.3	162.5	182.5	190.5	204.2	193.4	213.8	213.8	238.9	241.7	235.2	293.5	309.2
64	-109	179.1	168.3	182.2	198.3	205.7	202.7	213.7	217.7	239.8	252.9	239.9	292.3	312.3
65	-117	174.9	161.0	194.4	151.1	184.9	158.8	199.9	178.5	224.1	233.3	210.9	298.2	323.2
65	-116	176.7	160.3	196.5	162.0	186.8	170.4	204.0	191.7	227.2	233.8	224.2	298.6	316.9
65	-115	178.8	159.6	195.8	163.2	191.5	170.6	209.3	201.4	228.5	230.0	237.0	298.8	313.5
65	-114	180.8	159.0	194.7	164.2	200.4	170.0	216.1	198.5	234.5	227.1	251.8	298.8	312.6
65	-113	183.2	159.8	193.4	164.0	208.7	170.2	221.9	203.5	240.6	228.3	252.0	298.7	313.2
65	-112	185.5	161.3	191.0	169.5	208.0	183.0	219.9	208.3	240.1	230.1	244.2	296.6	314.2
65	-111	188.3	165.3	189.6	181.6	202.7	197.1	213.8	217.8	237.7	233.2	242.5	294.9	315.7
65	-110	192.7	170.7	188.9	200.7	206.8	202.8	216.1	219.5	239.9	239.6	243.4	294.9	317.2
65	-109	197.3	178.3	189.2	206.2	213.4	208.5	221.5	215.4	245.4	249.1	244.6	295.1	316.6
	Mean	175.4	159.5	182.0	170.9	197.1	178.6	210.5	195.8	230.7	224.6	226.1	294.3	314.2
	Median	174.9	159.6	182.3	169.3	199.0	178.1	213.8	196.0	233.7	228.5	230.9	294.9	312.6

Snow density

Long-term-average snow density estimates for the NGSR are shown in Table 2. These values were extracted from a gridded national database based on the historical snow course record (Brown *et al*., 2003). The gridded snow density data in Meteorological Service of Canada (2000) are mid-month and end-of-month mean snow density values on a $1^o \times 1^o$ grid. Annual average densities were estimated as the average of all values between November 15th and May 15th. Figure 11 summarizes the snow density data for all grid points located in the NGSR shown in Table 2, and average density values were used in simulations. From Meteorological Service of Canada (2000):

> "A database of gridded snow density normals was created from the snow course data. Grids were created for the 1st and 15th of the month between November 15th and May 15th inclusive. There was insufficient data to create grids before November 1st or after May 15th. All measurements were used which were within one week of the date of calculation. Snow densities were averaged over the entire period of record for all stations with at least five years of measurements for the calculation date. Average snow densities were then interpolated to a 200-km grid using the Shepard interpolation routine. Although snow course stations do not fully represent the actual topographical range of the Canadian terrain, snow density is a smooth variable and can be interpolated across topography more successfully than snow depth or SWE."

Analysis

Temperature and degree-days

For multi-year studies of permafrost conditions, the annual temperature cycle can be converted to a sine wave that retains the correct values for FDD_{Ann} and TDD_{Ann}. For an air temperature wave with amplitude A (i.e. an annual temperature range of 2A) and mean T_{Ann} (= MAAT), temperature T at time t (ignoring the phase of the wave) is:

$$T(t) = T_{Ann} + A\sin(2\pi t / P) \tag{1}$$

where t = time; A = air temperature amplitude; T_{Ann} = mean annual temperature (MAAT); P = Period (365 days). The surface temperature first reaches 0°C at time t_0, defined as:

$$t_0 = \left(P \big/ 2\pi\right)\sin^{-1}\left(-T_{Ann} \big/ A\right) \tag{2}$$

Thawing ends (and freezing begins) at $t = (P/2) - t_0$ and freezing ends at $t = P + t_0$, so that the seasonal freezing and thawing degree-day totals for this sine wave are:

$$FDD_{Ann} = -\int_{\frac{P}{\pi}-t_0}^{P+t_0} T_{Ann} + A\sin(2\pi t / P)\partial t \tag{3}$$

$$TDD_{Ann} = \int_{t_0}^{\frac{P}{\pi}-t_0} T_{Ann} + A\sin(2\pi t / P)\partial t \tag{4}$$

Letting $t_U = P/2 - t_0$, eqn. 4 resolves to:

$$TDD_{Ann} = \left(T_{Ann} \cdot t_U - \left(\frac{A \cdot P}{2\pi}\right)\right) 2\pi \cos\left(\frac{t_U}{2\pi P}\right) - \left(T_{Ann} \cdot t_0 - \left(\frac{A \cdot P}{2\pi}\right)\right) 2\pi \cos\left(\frac{t_0}{2\pi P}\right) \quad (5)$$

FDD_{Ann} can be calculated from MAAT and TDD_{Ann}, given that MAAT = (TDD_{Ann} – FDD_{Ann})/365. For example, Figure 6a shows the Yellowknife annual daily-mean temperature cycle for 2009, with the equivalent sine wave included (MAAT = -4.42°; FDD_{Ann} =3365; TDD_{Ann} =1753; A = 21.4°; Figure 6b shows that the sine wave provides a reasonably accurate approximation of the multi-year average daily mean air temperature). Using this approach, the 66 year degree-day time series in Figure 3b-c can be recreated within the model using means (Figure 3a) and amplitudes (Figure 6c).

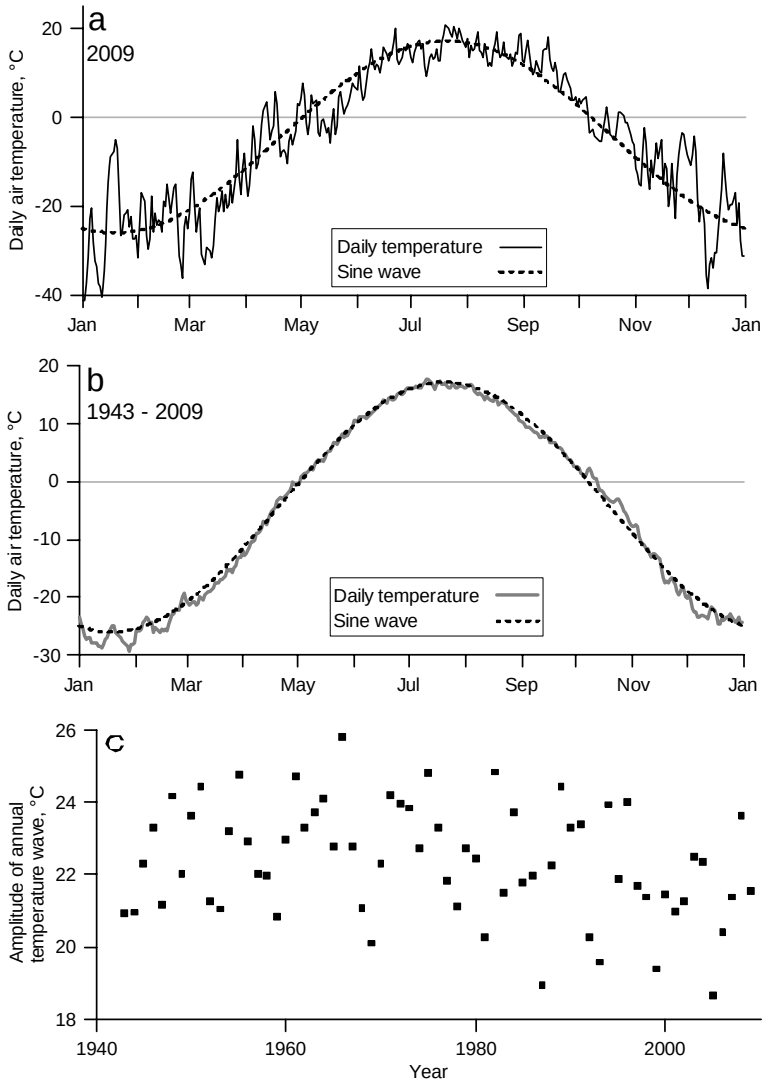

Figure 6. Air temperature data for Yellowknife, Northwest Territory, Canada: a) annual cycle of daily mean for 2009, with equivalent sine wave included; b) annual cycle of daily mean based on multi-year averages for 1943-2009, with equivalent sine wave included; c) trend of annual sine wave amplitudes calculated from FDD and TDD in (Figure 3 b and c).

Figure 7a shows the 2009 thaw-season daily air temperatures together with the thaw-season part of the sine wave (note that season dates have been shifted by about 11 days compared to Figure 6a so that the beginning of the thaw season coincides in the two time series). Figure 7b shows simulated seasonal active layer development using these temperatures with a typical Yellowknife-area peatland substrate, obtained with the finite element model TONE (model details below). Results show that the sine wave simulates active layer development reasonably well over the course of the thaw season, never departing from the results using daily temperatures by more than 0.05 m. Figure 7c shows the same results as 7b, plotted as a function of accumulated TDD: in this case, thaw depth results are consistently within 0.01 m, suggesting that the discrepancy in thaw depth over time in Figure 7b is primarily due to the timing of TDD accumulation. The maximum annual AFTT differs between the curves due to the early termination of the thaw season by a brief cold period in the simulation with daily variability. Additional simulations (not presented here) with simple step and saw-tooth temperature functions gave essentially the same active layer development curves shown in Figure 7c.

Snow cover

The properties of snow cover change continuously, from the start of snow accumulation in late autumn or early winter until its disappearance in spring, with variations that influence its effect on the ground thermal regime (Zhang, 2005). The challenge that snow cover presents for permafrost-

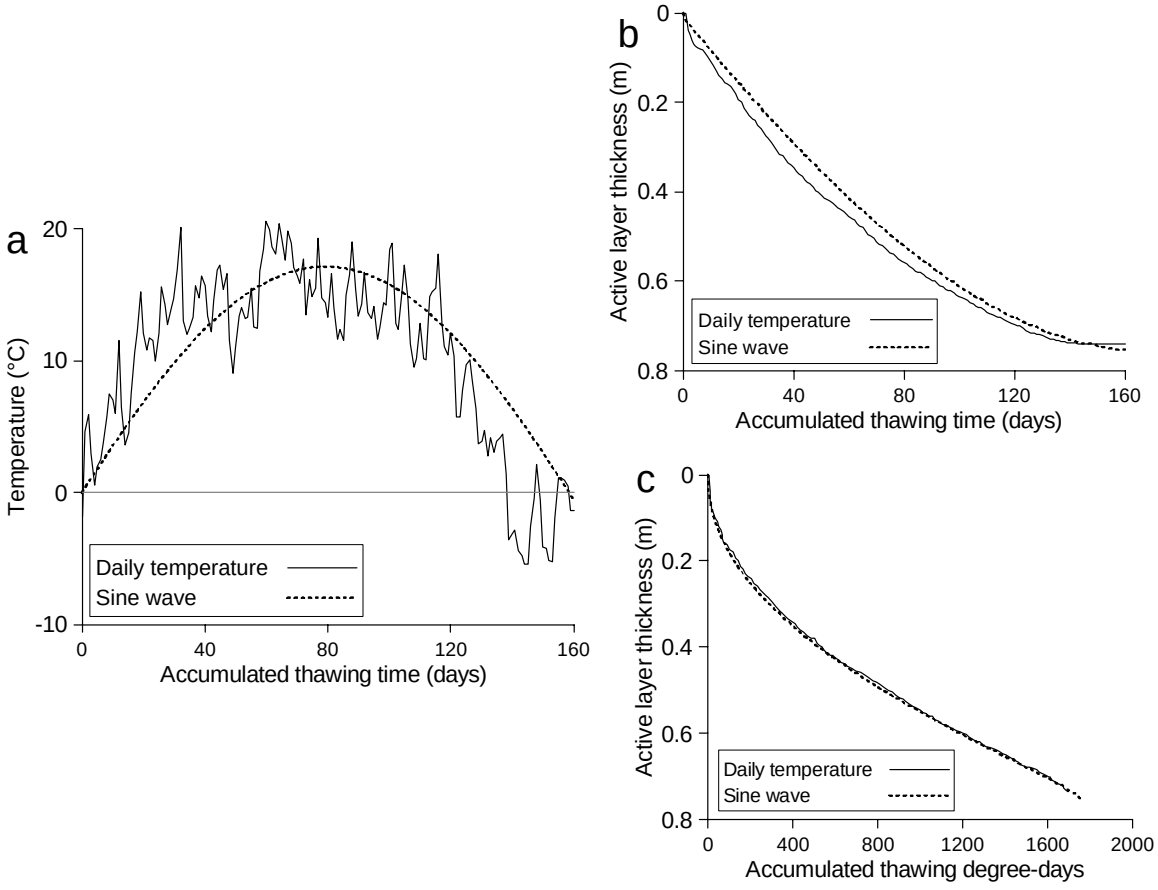

Figure 7. a) Simulated seasonal active layer development using thawing season air temperature data of Figure 6a, and with equivalent sine wave; b and c) simulated active layer development of (a) plotted versus accumulated thawing time (b) and degree-days (c).

climate models is to describe this variability in a way that allows it to be used in predicting its effect on permafrost temperature. In permafrost models, the thermal resistance of the snow pack determines its thermal effect rather than its thickness alone.

A snow cover is established when snow accumulates at a rate greater than can be ablated from above by energy supplied by radiation and local advection, or from below by conduction of heat from the ground (Groisman and Davies, 2000). Wind can redistribute snow, scouring it from exposed areas and re-depositing it in sheltered areas. Deposition and redistribution under high winds can result in extremely hard, high-density "wind-slab" snow (Sturm *et al*., 1995). As snow accumulates the weight of the snow overburden results in mechanical compaction (Sturm and Holmgren, 1998). Thawing episodes in the winter can collapse the pore spaces in warm, wet snow and may produce refrozen ice layers (Sturm *et al*., 1995). Strong temperature gradients between the top of the snow cover and the ground surface can produce depth hoar, "a type of snow dominated by large, ornamented, delicately connected single crystals that grow when large temperature gradients prevail in the snow cover and induce large water vapour density gradients" (Arons and Colbeck, 1995). Sturm *et al.* (1995) suggest that while a thin basal depth hoar layer is common in tundra snow covers, in taiga environments it may comprise 50 to 80% of the total snow depth by late winter. At the start of the thawing season the snow cover warms to the melting point, and ablates with energy supplied from the atmosphere and the ground (Pomeroy, 1998).

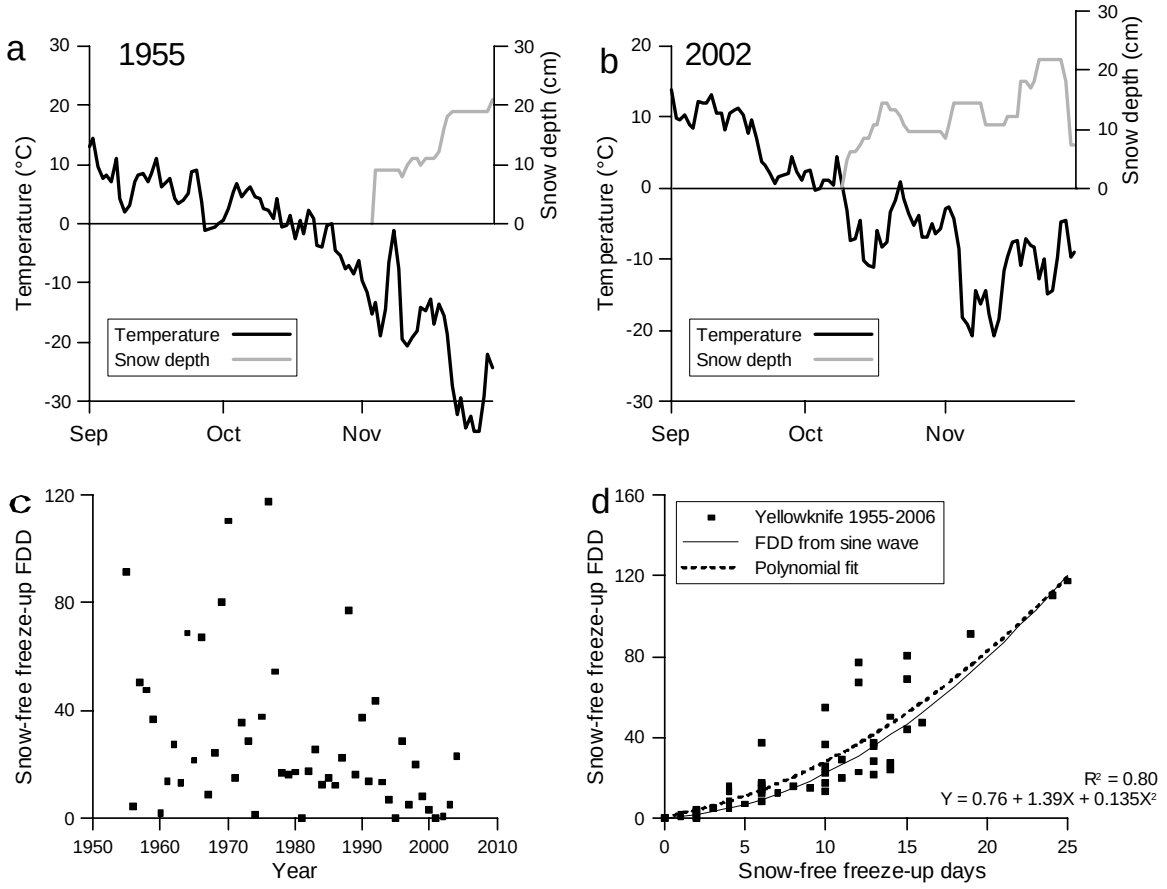

Figure 8. a) Daily mean air temperature and snow depth at the beginning of the freezing season, 1955; b) Daily mean air temperature and snow depth at the beginning of the freezing season, 2002; c) 1955-2006 trend in snow-free total FDD for the beginning of the freezing season; d) Snow-free FDD totals for the beginning of the freezing season as a function of the duration of the snow-free period.

Snow cover initiation

The relationship between the beginning of the snow accumulation season and the beginning of the freezing season is critical to the ground thermal regime (Goodrich, 1982, Ling and Zhang, 2007). Riseborough (2004) found that delayed snow cover reduces ground temperatures far more than can be attributed to the increase in surface FDD alone: earlier active layer freeze-up affected the ground thermal regime for the rest of the season. Figures 8a and 8b shows extreme examples from the Yellowknife climate record where snow cover and freezing conditions arrive simultaneously (year 2002, Figure 8b), or after a delay of two weeks (year 1955, Figure 8a). Figure 8c shows the trend in snow-free freeze-up FDD for the climate record.

Figure 8d shows the relationship between the FDD total and the length of the snow-free period at the beginning of the annual freezing season for the Yellowknife climate record. Data for individual years of the record are shown as points, with a polynomial fit through the data shown as a dashed line. Also included is the FDD accumulation expected for a sine wave (solid line), calculated for the mean FDD and TDD using the mean and amplitude for the Yellowknife data. The approximate agreement between the polynomial fit and the theoretical result suggests that the use of a specified time delay in conjunction with the sine wave produces the appropriate FDD value.

Figure 9 shows the distribution of snow-free FDD at the beginning of the annual freezing season for the Yellowknife climate record. The mean length of the snow-free freeze-up period is 8.9 days with a standard deviation of 5 days; the mean FDD for this period is 28.3 degree-days, with a standard deviation of 28.5 degree-days.

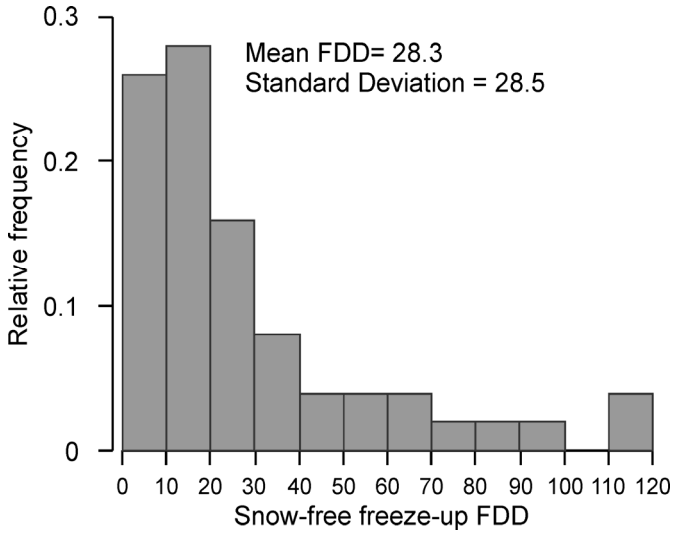

Figure 9. Distribution of FDD totals for the snow-free period at the beginning of the freezing season.

Snow accumulation

Based on an analysis of the climate record for Barrow, Alaska, Zhang *et al*. (1996) characterized the snow accumulation rate as a parabolic function:

$$Z_t = Z_{\max}\left(\frac{t - t_{init}}{t_{\max} - t_{init}}\right)^{0.5} \tag{6}$$

where t = time; Z_t = snow depth at time t; $Z_{\max}$ = maximum snow depth; t_{init} = time of snow cover initiation; $t_{\max}$ = time of maximum snow depth. Osokin *et al*., (2000) found that the exponent in equation (6) varied between 0.4 and 0.6 for a number of climate stations in Russia. Zhang *et al*. (1996) modelled deflation of the snow pack at the end of the snow cover season using a similar function:

$$Z_t = Z_{\max}\left(\frac{t - t_{\max}}{t_{end} - t_{\max}}\right)^{1.5} \tag{7}$$

Figure 10a shows the annual snow depth record for all years of the Yellowknife record, superimposed. Figure 10b shows the mean and median snow depth from these data, together with two possible accumulation functions. Both use the average snow season delay of Figure 4a and the maximum of the median snow depth curve of Figure 10a. The exponent 0.6 function reaches maximum at the mean date of maximum snow depth from the climate record, with end-of-season deflation using equation 7, while the exponent 0.5 function reaches the maximum at the end of the accumulation season (so that the snow disappears by ablation without deflation). The square root curve over-predicts snow depth early in the season and under predicts it late in the season, whereas using 0.6 for the exponent is closer to the data curve, albeit with extended periods of over and under prediction. Handling of the end-of-season snow cover is discussed in the section below on ablation.

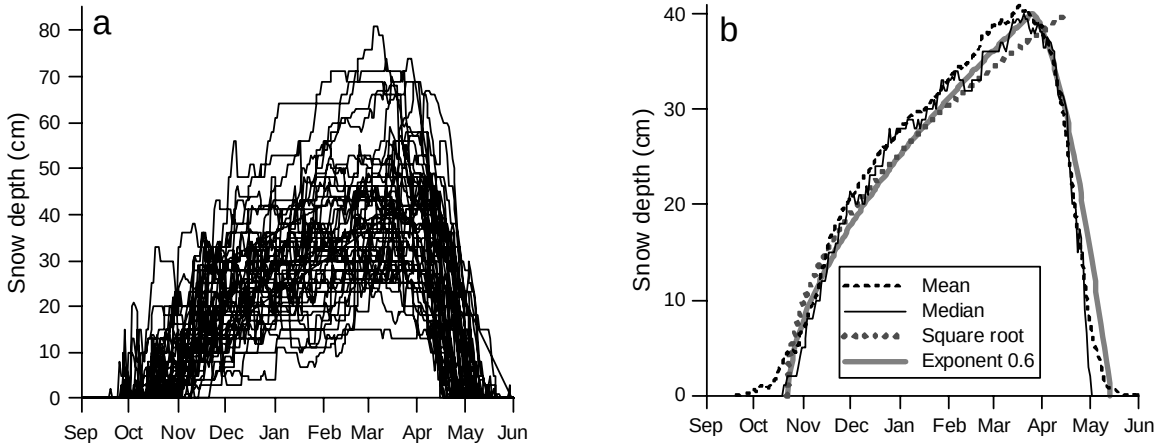

Figure 10. a) Yellowknife snow accumulation curves for individual years 1955-2005. b) Mean and median daily snow depth from data in (a), with different accumulation curves derived for seasonal maximum and freezing-season end, and with/without deflation at season end.

Snow density variation

Although many other factors have an influence, density is the most common parameter used to model the thermal properties of snow cover (Sturm *et al*., 1997). Snow naturally develops a layered structure as it undergoes compaction and metamorphism between discrete deposition events. Whereas many processes are critically dependent on the distribution of properties of the strata, the use of average density is usually sufficient for thermal studies (Colbeck, 1991).

Unfortunately, snow density (or snow water equivalent (SWE), the parameter which allow calculation of snow density from snow depth data) is not usually collected at meteorological sites. Although it is possible to estimate snowpack densities from precipitation data using a viscous compaction model such as Kojima (1967), this approach does not account for the development of depth hoar.

Brown *et al*. (2003) developed a Canada-wide grid of mean snow density at 15-day intervals over the winter season based on historical snow course record. Figure 11 shows the seasonal trend in snow density for the grid points within the NGSR. This was used to provide appropriate parameters for use in the model.

Snow ablation

Snow ablation is the object of many models used to predict melt water runoff. In the context of geothermal modelling however, snowmelt is important for the prediction of the end of snow cover, and the beginning of the ground surface layer thaw season. The freezing season at the ground surface usually ends when the snow cover is completely ablated. The principal snowmelt period at the end of winter may begin with the arrival of air temperatures above 0°C, or with sufficient incoming solar radiation to raise the temperature of the upper snow layers above freezing (Pomeroy and Brun, 2001). When snow melts at its upper surface, water percolates through the snow, refreezing if it encounters snow below 0ºC. This process of snowpack *ripening* continues

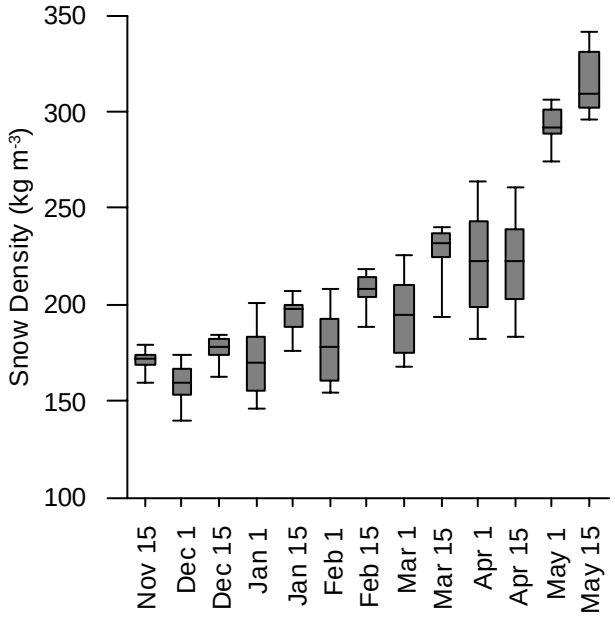

Figure 11. Seasonal trend in snow density for grid points near Yellowknife from the snow density database provided in MSC (2000).

until the whole snow cover is at the melting point. In ground that remains unfrozen under the snow cover, heat can be supplied to warm the snow from below as well. If the ground beneath the snow cover is frozen, ripening proceeds until the ground surface temperature is 0°C. Once the snow is isothermal at the melting point, energy is available for snowmelt. For ground thermal modelling purposes, the thickness and density profile of the ablating snow cover has a negligible effect once it has reached the "ripe" stage (isothermal at 0°C), since the ablation process keeps the ground surface temperature at 0ºC until the snow is gone. The simplest model for the ablation process (Pomeroy and Goodison, 1997) relates snowmelt to the thawing degree-day total:

$$SWE_A = M_f \, TDD \tag{7}$$

where SWE_A = ablated snow water equivalent, and M_f = melt factor, kg $m^{-2}TDD^{-1}$

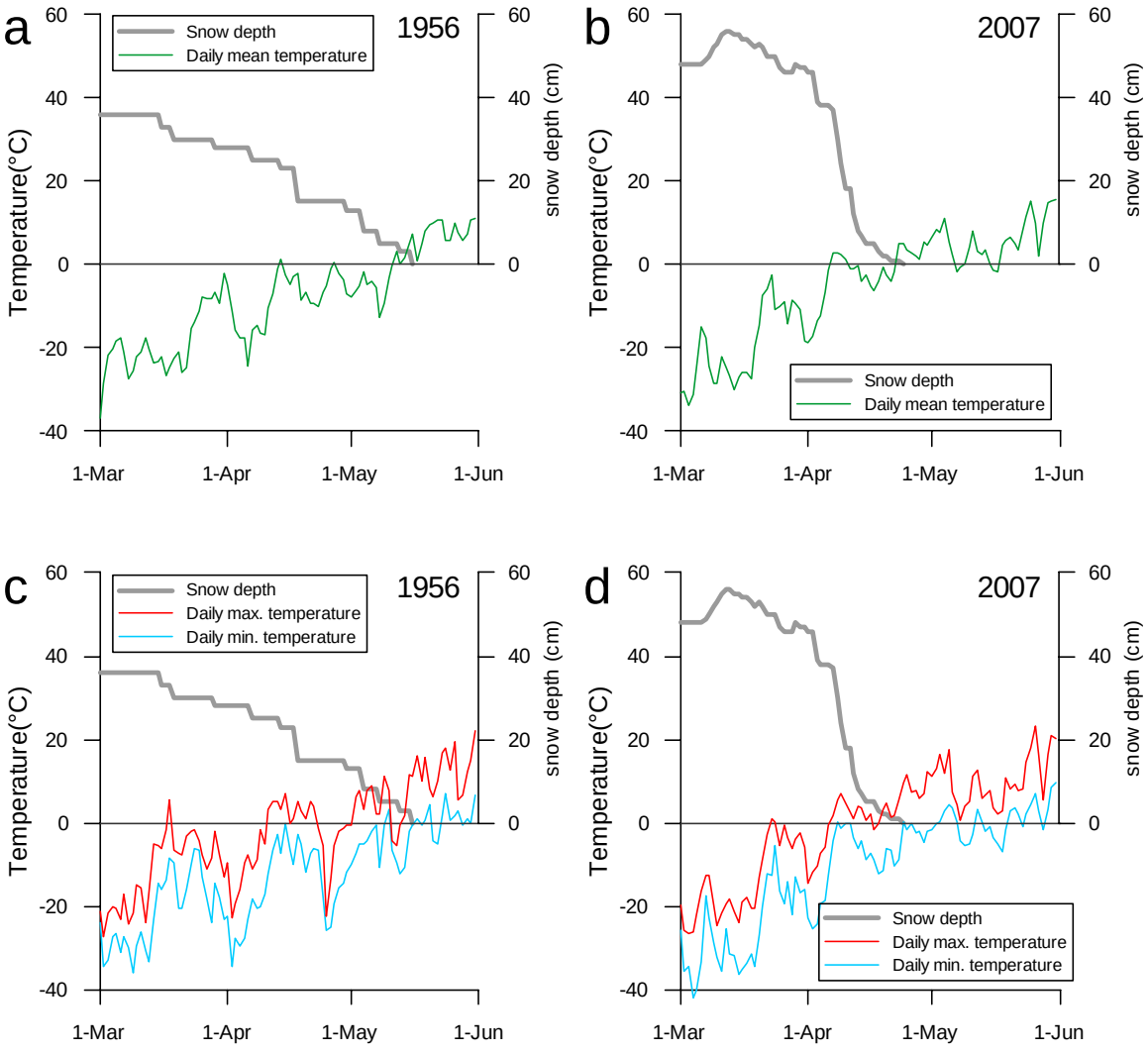

Figure 12. a) Daily mean air temperature and snow depth at the end of the freezing season, 1956; b) Daily mean air temperature and snow depth at the end of the freezing season, 2007; c) Daily maximum and minimum air temperature and daily mean snow depth at the end of the freezing season, 1956; d) Daily maximum and minimum air temperature and daily mean snow depth at the end of the freezing season, 2007.

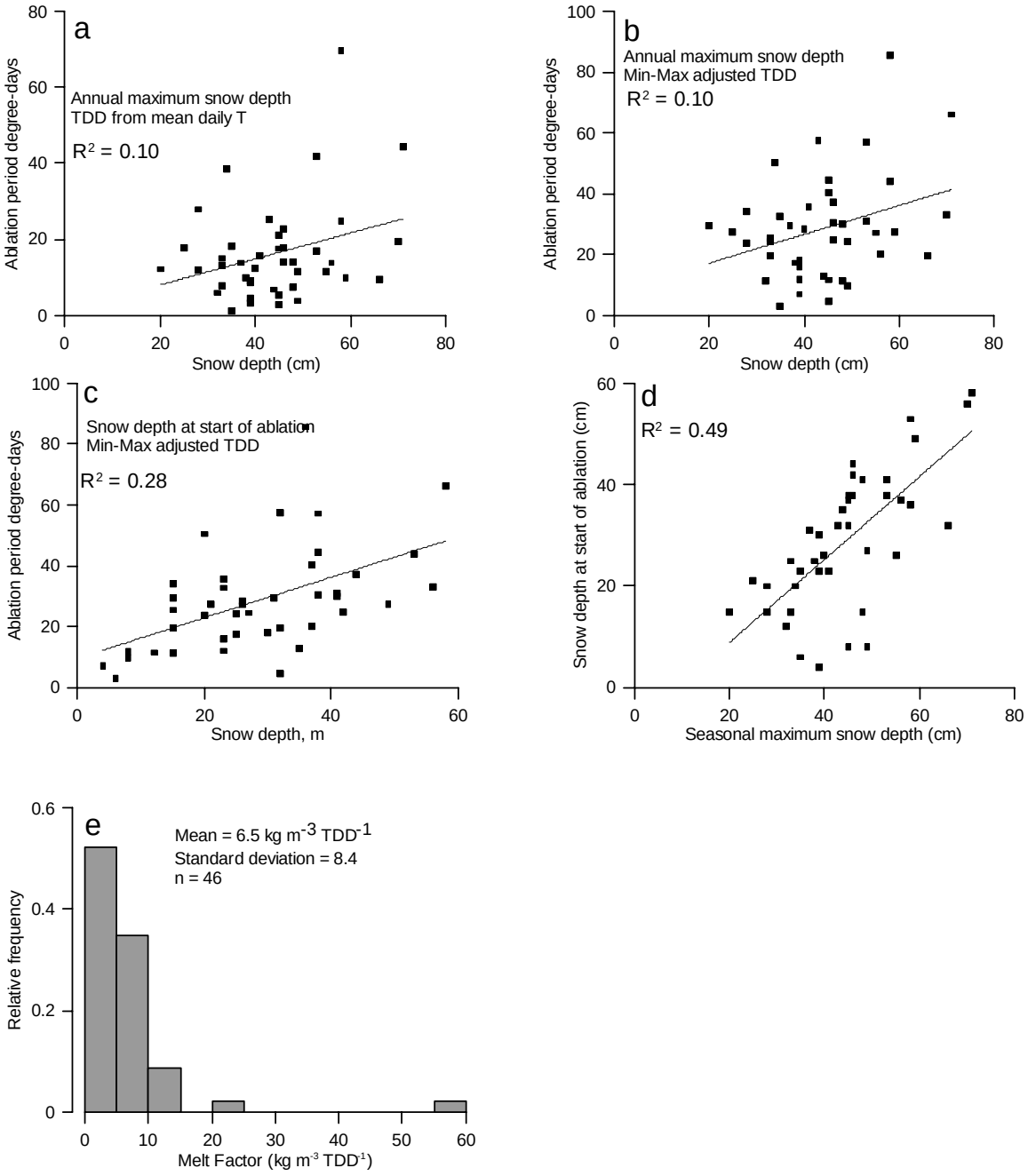

Figure 13. Using data for Yellowknife 1955-2005: a) Relationship between annual maximum snow depth and ablation-period TDD derived from daily mean temperature; b) Relationship between annual maximum snow depth and ablation-period TDD derived from daily maximum & minimum temperature; c) Relationship between snow depth at start of ablation and ablation-period TDD derived from daily mean temperature; d) Relationship between snow depth at start of ablation and ablation-period TDD derived from daily maximum & minimum temperature; e) Distribution of calculated M_f from data in (a), assuming a snow density of 212. kg m-2 (mean for April 15 in Figure 7) derived for seasonal maximum and freezing-season end.

The snow cover disappears at the start of the thaw season as a result of the ablation process, in which radiant and convective energy from the atmosphere is sufficient to melt the snow. On average, however, the Yellowknife snow cover reaches its maximum thickness on March 10, or about 73% of the way through the freezing season, about a month before the average date that the daily mean air temperature rises above 0°C (April 11). Figure 12 shows the progression of snow depth at the end of the freezing season in two years, combined with plots of either daily mean temperature (12a and 12b) or daily minimum and maximum (12c and 12d). The data indicate that the deflation process begins several weeks before the ablation process begins, suggesting that it is not sufficient to rely on the ablation process alone to parameterize the evolution of the snowpack at the end of the snow season.

Numerical thermal models with relatively simple routines to handle snow evolution (such as TONE, the model used in the next section of this report) use M_f to ablate the snow. For a given time step, snow cover loss is modelled using the calculated SWE_A mass to determine a decrease in snow layer thickness, converted to layer thickness using the snow density. Figure 13a shows the relationship between snow depth at the end of the freezing season, and the accumulated TDD for the period of ablation. The relationship is weak, in part because the density of the snow cover is unknown, because mean daily temperatures do not capture the melt that can occur on days with mean air temperature below 0°C but a high above 0°, as well as the effect of rising temperatures on the accelerated mechanical densification of the snow pack. Figure 13e shows the distribution of values for M_f based on these data, with the assumption that the snow in all years has a density equal to the regional mean for April 15 (from Figure 11).

Climate parameter sensitivity analysis

Prior to an analysis of substrate properties, a sensitivity analysis was performed to evaluate the relative importance of the snow cover parameters on the mean annual ground temperature. The particular parameter choices for this study were determined in part by the functional capabilities of the numerical model being used. For permafrost (and active layer) modelling, retaining accurate values for TDD_{Ann} and FDD_{Ann} is the most important aspect of parameterizing the surface climate. While it is relatively straightforward to evaluate the effect of assumptions in the air temperature regime, it is much more difficult to perform this type of analysis on the effect of simplifying the snow accumulation regime. With the temperature regime, the effects being removed are at time scales shorter than the annual cycle, but the overall thermal climate is captured by the annual freezing and thawing degree day totals. For the snow cover however, the simplified representation of any individual annual accumulation is not captured by the parabolic function, so that the effect of the snow cover is almost certainly misrepresented in any single year. Riseborough (2007) demonstrated that long-term (multi-year) simulations with variability in a suite of parameters produced a long-term average thermal regime that was very close (mean annual temperature at the base of the active layer within 0.15°C) to the thermal regime of similar simulations without variability.

Riseborough (2004) found that snow accumulation at a number of Canadian arctic climate stations conformed reasonably well to the parabolic accumulation function of equation 6. The analysis did not include an evaluation of the seasonal timing of the maximum snow depth, although the data suggest that this varied from about 65% to 90% of the freezing season length. The climatology of this effect needs to be evaluated to allow the best empirical fit, and application of equation 7.

Table 3 summarizes a preliminary sensitivity analysis evaluating the effects of the simplifying assumptions on the mean ground temperature at the base of the annual freezing/thawing layer. All simulations had the same substrate (1 m saturated peat over 8 m clay over bedrock), and were run for a minimum of 100 annual cycles to approach equilibration. Surface climates were based on 1955-2006 multi-year averages, and were either daily average temperature and snow depth ("Data" in Table 3), or a degree-day appropriate sine wave ("Sine") with a range of snow cover treatments. Differences in mean annual ground temperature (MAGT) allow a ranking of the relative importance of the various simplifications to the accuracy of model results.

The simulations based on daily data (1 & 7 in Table 3) were closest in temperature to the simplified climate simulations with a snow cover most closely resembling the daily data (6 & 9), although simulations with the simplest snow cover (4 & 10) differed from 1 and 7 by 0.1°C or less. The largest temperature differences (>1°C) are between simulations with constant (1-6) and time varying (7-12) snow cover density.

Implications for model development

The model used for this analysis (described in the following section) was modified for use with known interannual snow depth and temperature variability (the prior version generated variability stochastically). The modified version of the model has the flexibility to explore the sensitivity of results to seasonal snow density variations and snow cover deflation for an unchanging climate, but cannot accommodate these seasonal variations in combination with interannual variation. Based on the findings of the sensitivity analysis above, further modification of the model allowing for the specification of these seasonal properties of the snow cover is required.

Table 3. Results of sensitivity analysis

	Air Temperature	Snow depth exponent	Timing of max. snow [1]	Deflate Snow ? [2]	Snow density	MAGT (°C)
1	Data	Data	Data	Data	Constant	0.92
2	Sine	0.5	0.75	Yes	Constant	1.29
3	Sine	0.5	0.75	No	Constant	1.43
4	Sine	0.5	0.99	No	Constant	0.85
5	Sine	0.4	0.75	Yes	Constant	1.81
6	Sine	0.6	0.75	Yes	Constant	0.94
7	Data	Data	Data	Data	f (time)	2.03
8	Sine	0.5	0.75	Yes	f (time)	2.34
9	Sine	0.5	0.75	No	f (time)	2.37
10	Sine	0.5	0.99	No	f (time)	1.93
11	Sine	0.4	0.75	Yes	f (time)	2.58
12	Sine	0.6	0.75	Yes	f (time)	1.97

[1] Timing of snow cover maximum depth relative to the length of the freezing season

[2] Is snow depletion at the end of the snow season determined by a reverse-square-root function ("Yes") or by ablation ("No")

ONE-DIMENSIONAL MODELLING

Model description

Numerical results were generated using Goodrich's discontinuous finite element model TONE (developed by Laurel Goodrich of the National Research Council of Canada, and evaluated in Bouchard, 1990 and Riseborough, 2004). In TONE, the latent heat of fusion is accounted for using apparent heat capacity; at each simulation time step, thermal conductivity and apparent heat capacity within each element are averaged based on the temperature profile, improving accounting for the total latent heat and abrupt temperature-dependent changes in thermal properties. Accommodating the distribution of thermal properties across each element improves results in soils that exhibit strong temperature dependence in thermal properties due to the freezing characteristic; significant transitions over small temperature changes are not lost between points in the calculation mesh.

In this simulation study, we assumed that the initial ground thermal condition was in equilibrium with the normal climate of 1971-2000 from Yellowknife. Air temperature was modelled as a sine-wave with mean and amplitude set to match station values for freezing-degree-days (FDD) and thawing-degree-days (TDD) (Riseborough *et al*., 2012). When no snow is present, TONE uses the air temperature and a regional N-factor of 0.8 to calculate ground surface temperature (GST) values. Snow cover was initiated eight days after the surface temperature dropped below 0°C (based on weather station averages), and accumulated with the square root of time. The annual maximum snow cover depth is based on the climate normal data and occurs just before the onset of ablation, which is controlled by thawing-degree-days at a rate of 1.5 kg m^{-2} per degree-day (Riseborough and Smith, 1993). The snow density was assumed to be 220 kg m^{-3} based on regional studies (Brown *et al*., 2001). TONE adds additional elements when snow is present, automatically ensuring a minimum Fourier number of 0.1. Ground surface temperature when snow is present is not a boundary condition, but is calculated based on heat flow through the snow and the ground. To accommodate the annual snow cover, simulations ran from mid-year to mid-year (starting on July 1st).

Thermal properties of the soil and snow used in the simulations are given in Table 5. Simulations were run with a time step of 40 minutes, with an element size of 0.02 m at the ground surface, increasing to about 0.15 m at 20 m, increasing exponentially to 25 m at the bottom of the grid (500 to 510 m) depth. A 70 mWm^{-2} geothermal heat flux was used as the lower boundary condition for all simulations, based on the regional value (Majorowicz and Grasby, 2010).

To establish periodic equilibrium, simulations were run with the 1971-2000 normal climate data for hundreds of cycles until the difference in temperature profiles between cycles was less than 0.001 °C. The final output became the initial condition for 1955-2006. During this timeframe, air temperature sine waves and maximum snow cover depths were generated each year from the climate station data, adjusting the length of the snow cover season annually.

Yellowknife substrate profiles and properties

While climatic parameters have a large effect on the thermal regime, substrate properties also play a significant role, primarily through the thermal offset effect (Smith and Riseborough, 1996, 2002) and the effect of soil moisture on the storage of heat from active layer thaw beneath the snow cover (Karunaratne *et al*., 2008). In the NGSR, ground temperatures are generally close to 0°C, so that variations in ground temperature due to substrate conditions are sufficient to determine whether permafrost is present or stable under current climatic conditions. Based on borehole logs collected along the Yellowknife- Behchoko highway and adjacent terrain (Wolfe *et al.*, 2011), a number of soil profiles (Table 4; Figures 15 and 16) were created to represent a range of typical local environments for use in simulations. Typical conditions were assumed to be a thin veneer of sand or ice-rich silty clay 0 – 10 m thick over bedrock, usually covered by an organic soil layer 0.1 to 2 m thick. Note that the clay substrate material is labelled as "wet clay" (with 60% water or ice by volume), since "ice-rich" would only be an accurate label or for this material in the frozen state. In the sensitivity analysis, most simulations included 4 m of mineral soil and 0.2 m of organic cover, with additional simulations without mineral soil or with soil 9 m thick, and some with no organic cover; the effect of fully saturated and unsaturated surface organic layer properties were also explored. The thermal and physical properties of the substrate materials used in simulations are shown in Tables 5 and 6, with the temperature dependent properties of the wet silty clay shown in Figure 14. As results indicated a strong dependence on organic layer properties, a suite of simulations examining the combined effects of organic layer thickness (OLT) and saturation over the three representative substrates (sand, silty clay, bedrock) was also undertaken.

Simulation results for the various substrates are summarized below using two parameters: the annual maximum freezing or thawing layer thickness (AFTT) and the mean annual temperature at the bottom of the freezing / thawing layer. In most conditions, the bottom of the active layer corresponds to the top of permafrost. When permafrost is degrading, or in a year following the development of an exceptionally deep active layer, a layer of soil may remain unfrozen through the winter (referred to as a *talik*). In these cases the term TTOP is used, but refers to the mean annual temperature at the base of the active layer; the mean annual temperature at the top of permafrost (i.e. at the base of the *talik*) in these cases will be very close to 0°C.

Table 4. Stratigraphies used in simulation modelling.

Profile	Label	Thickness (m)
Bedrock	Bedrock	500
Clay over bedrock	Wet clay	4
	Bedrock	500
Dry sand over bedrock	Dry sand	0.1
	Moist Sand	3.9
	Bedrock	500
Low moisture organic over bedrock	Low moisture organic	0.2
	Moist Organic	0.4
	Saturated Organic Base	0.4
	Bedrock	500
Low moisture organic over clay over bedrock With 1 m sand at base	Low moisture organic	0.2
	Moist Organic	0.4
	Saturated Organic Base	0.4
	Wet clay	3
	Saturated sand	1
	Bedrock	500
Low moisture organic over 9 m clay over bedrock	Low moisture organic	0.2
	Moist Organic	0.4
	Saturated Organic Base	0.4
	Wet clay	4
	Bedrock	500
Low moisture organic over clay over bedrock	Low moisture organic	0.2
	Moist Organic	0.4
	Saturated Organic Base	0.4
	Wet clay	4
	Bedrock	500
Low moisture organic over sand over bedrock	Low moisture organic	0.2
	Moist Organic	0.4
	Saturated Organic Base	0.4
	Moist sand	4
	Bedrock	500
Saturated organic over bedrock	Saturated Organic Bulk	1
	Bedrock	500
Saturated organic over clay over bedrock With 1 m sand at base	Saturated Organic Bulk	1
	Wet clay	3
	Saturated sand	1
	Bedrock	500
Saturated organic over clay over bedrock	Saturated Organic Bulk	1
	Wet clay	4
	Bedrock	500
Saturated organic over 9 m clay over bedrock	Saturated Organic Bulk	1
	Wet clay	4
	Bedrock	500
Saturated organic over sand over bedrock	Saturated Organic Bulk	1
	Saturated sand	4
	Bedrock	500
Saturated sand over bedrock	Saturated sand	4
	Bedrock	500

Table 5. Soil physical and thermal properties used in simulation modelling

Layer Label	Dry Bulk Density kg m^{-3}	Porosity %	Gravimetric Moisture %	Volumetric Moisture %	Quartz Fraction %	k_F $Wm^{-1}K^{-1}$	k_T $Wm^{-1}K^{-1}$
Bedrock	2544	4	2	4	50	3.834	3.633
Dry sand	1590	40	5	8	80	0.972	1.284
Moist Sand	1590	40	13	20	80	2.102	1.875
Saturated Sand	1590	40	25	40	80	3.968	2.312
Wet clay	1060	60	57	60	0	1.800	0.942
Low Moisture Organic	130	90	308	40	0	0.246	0.146
Moist Organic	260	80	231	60	0	0.634	0.304
Saturated Organic Base	390	70	180	70	0	1.210	0.470
Saturated Organic Bulk	260	80	308	80	0	1.477	0.501

Table 6. Temperature dependent unfrozen water content (volume fraction) and thermal conductivity ($Wm^{-1}K^{-1}$) for wet clay soil used in simulation modelling.

Temperature (°C)	Unfrozen Water (volume fraction)	Conductivity ($Wm^{-1}K^{-1}$)
-100.000	0.0470	1.991
-40.000	0.0470	1.991
-29.235	0.0518	1.978
-21.355	0.0571	1.965
-15.586	0.0630	1.950
-11.363	0.0695	1.933
-8.272	0.0766	1.915
-6.009	0.0846	1.895
-4.352	0.0935	1.873
-3.140	0.1035	1.849
-2.252	0.1147	1.822
-1.602	0.1275	1.791
-1.126	0.1422	1.757
-0.778	0.1595	1.718
-0.523	0.1804	1.671
-0.337	0.2068	1.614
-0.200	0.2430	1.539
-0.100	0.3013	1.426
0.000	0.6000	0.942
10.000	0.6000	0.942

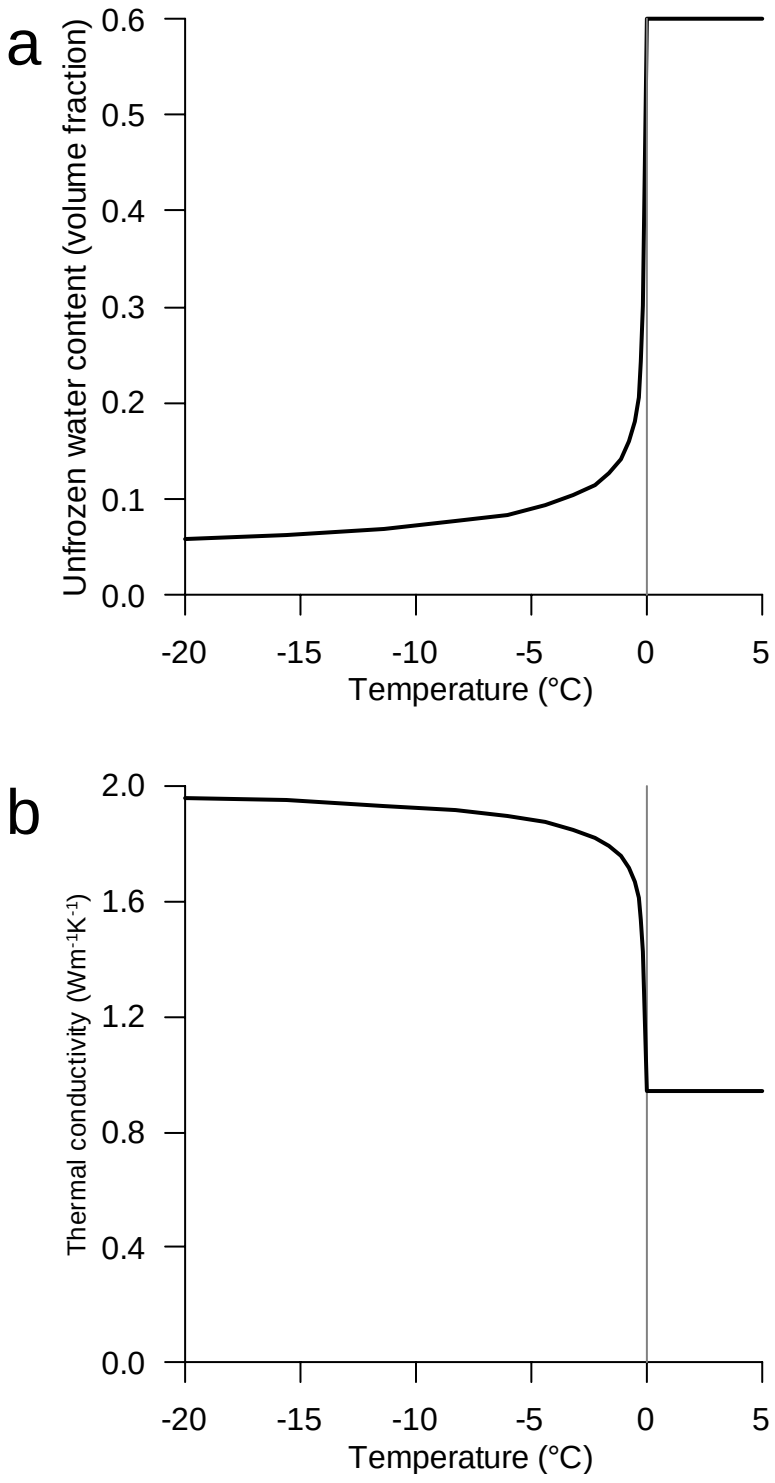

Figure 14. a) Temperature dependent unfrozen volumetric water content (fraction); b) Temperature dependent thermal conductivity ($Wm^{-1}K^{-1}$) for wet clay soil used in simulation modelling.

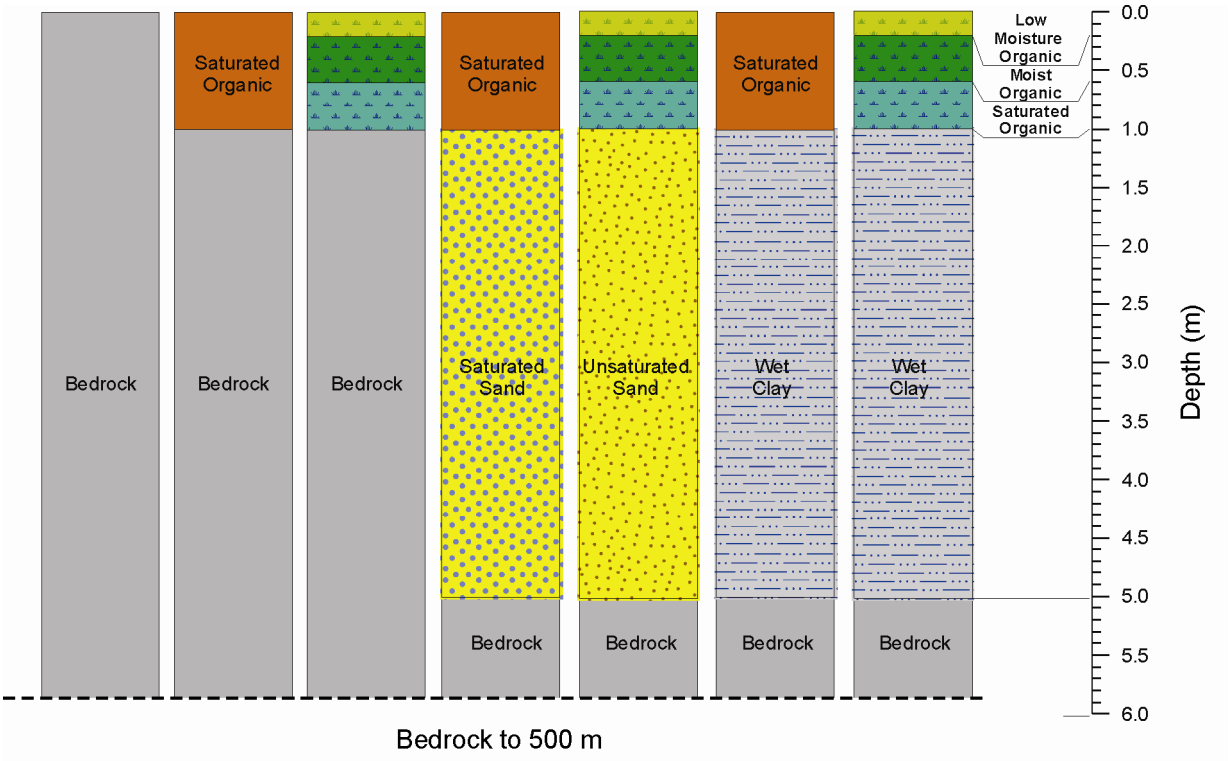

Figure 15. Stratigraphic profiles of representative terrain types used in simulation modelling.

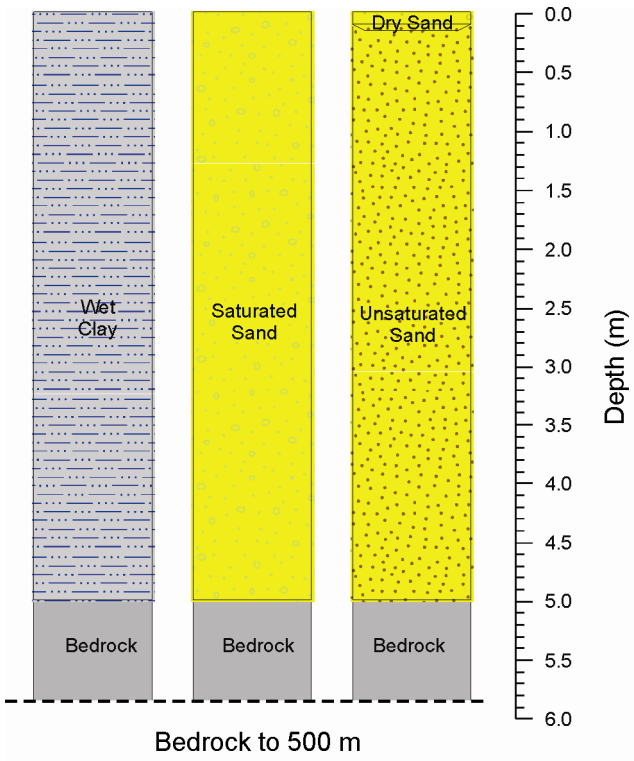

Figure 16. Stratigraphic profiles of special terrain types used in simulation modelling.

Modelling results

Most results are presented as box-whisker plots, which show maximum, upper quartile, median, lower quartile and minimum values for the 1955-2006 period for each case examined. In some cases multi-year averages for the 1955-2006 period are also shown. Because the recent climate trend has been toward higher temperatures (Figure 3), in most cases simulation AFTT and TTOP values for the most recent years are toward the high end of the distributions.

Typical profiles

Simulation results using typical substrate profiles are shown in Figure 17a (mean annual temperature at the base of the annual freezing/thawing layer - TTOP) and Figure 17b (AFTT); results are ordered by the long-term mean TTOP. Comparing mean annual temperatures, substrates topped with an unsaturated organic layer were the coolest, while sites with no surface organic layer were the warmest. The mineral substrate that was coldest or warmest was different for each of these groupings. Comparing annual maximum annual freezing/thawing layer thicknesses, sites with no mineral soil above bedrock had the deepest annual freezing/thawing layers by a large margin, while substrates with clay or sand had different rankings depending on the surface (organic layer) condition.

Figure 18 compares results for profiles with similar surface organic layers (20 cm of saturated or unsaturated material) over different thicknesses of the mineral soil layer (4 or 9 m thickness of wet clay or moist sand) above bedrock; in addition, cases with saturated and unsaturated organic material over wet clay layers (3 or 8 m thick) underlain by 1 m of sand above the bedrock are included. Mineral soil layers more than 4 m thick have a very small effect on the mean annual temperature (mean TTOP differences of less than 0.1°C for all unsaturated organic cases and the saturated organic with sand case, and less than 0.2°C for the saturated organic cases with clay). Differences in mean AFTT were negligible for the saturated and unsaturated organic case with sand (mean AFTT differences of less than 1 cm); for the wet clay cases, differences were about 7 cm for the unsaturated organic cases and up to 18 cm for the saturated cases. The large differences in annual freezing/thawing layer for the saturated organic wet clay cases are due to the combined effects of the proximity of the ground temperature to 0°C and the significant unfrozen water curve for the clay.

Varying organic layer thickness (OLT) and moisture content

Within the study area, a surface organic layer may be absent or as much as 4 m in thick (Wolfe *et al.*, 2011), and conditions vary from saturated to moist (possibly with an extremely dry upper surface). Results in Figures 17 and18 demonstrate the importance of the surface organic layer in controlling the annual thermal regime of the ground with large differences in permafrost temperature depending on whether the organic layer is saturated or unsaturated, present or absent. Variations in the thickness and degree of saturation of this layer probably control the distribution of permafrost in this region more than any other surface properties. The physical composition of the organic layer – its density, fibrous structure, etc – is also variable but is not considered in this study. Figures 19-21 show, for each substrate (clay, sand, or bedrock, respectively) the effect of variations in OLT (to a maximum thickness of 1 m) on the mean annual ground temperature and AFTT, for both saturated and unsaturated organic materials. The range of annual freezing/thawing layer depths in the box-whisker diagrams of Figures 19-21 varies widely across the range of organic layer thicknesses. Overall, annual freezing/thawing layer variability is greater with a thinner organic layer, although the range is widest where the mean TTOP is close to 0°C for the unsaturated cases.

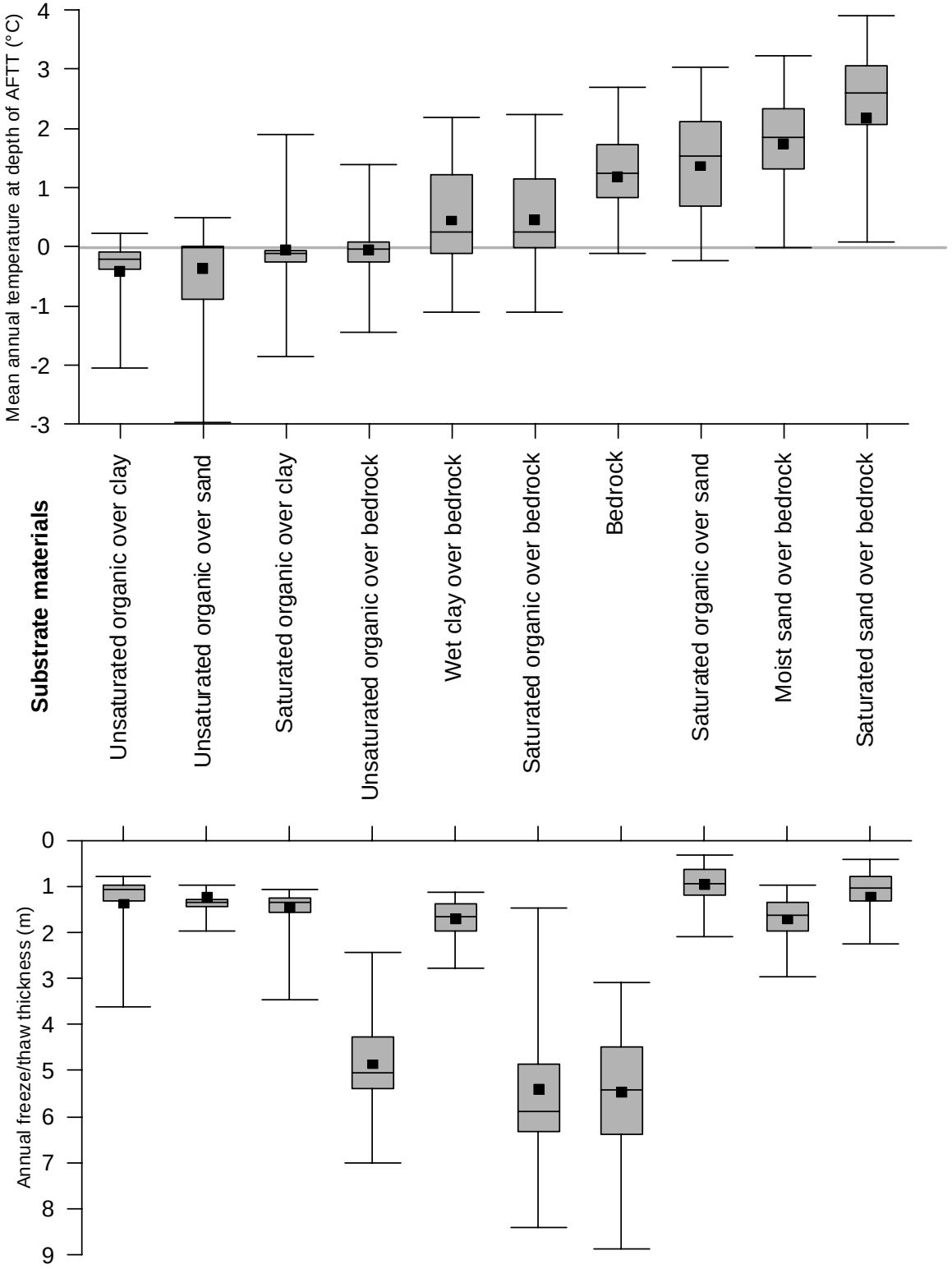

Figure 17. Results for representative terrain types, using 1955-2006 Yellowknife climate statistics with organic layers (saturated and unsaturated) 20 cm thick Square symbols indicate 51-year mean. a) Mean annual temperature at t the top-of-perennially frozen/unfrozen ground (TTOP). b) Simulated maximum annual freezing/thawing layer thickness (AFTT) values. Boxes and whiskers show maximum, upper quartile, median, lower quartile and minimum values for 1955-2006 for each thickness

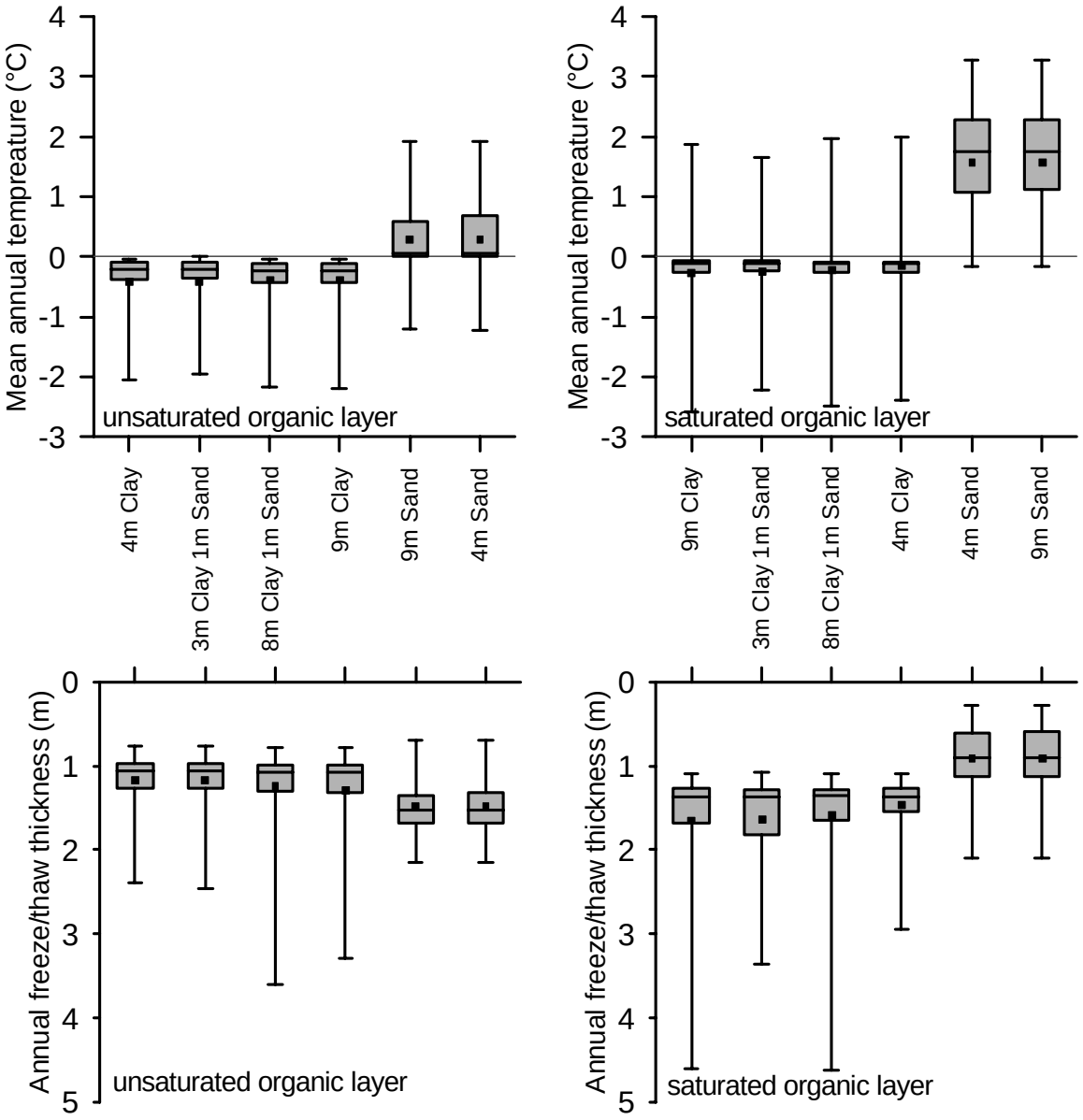

Figure 18. Simulated mean annual temperature at the top-of-perennially frozen/unfrozen ground (TTOP) and annual freezing/thawing layer thickness (AFTT) values for sand and clay substrates with various configurations, all with 20 cm organic layer (saturated and unsaturated), using 1955-2006 Yellowknife climate statistics (preceded by 300-year spin-up). Boxes and whiskers show maximum, upper quartile, median, lower quartile and minimum values for 1955-2006 for each thickness.

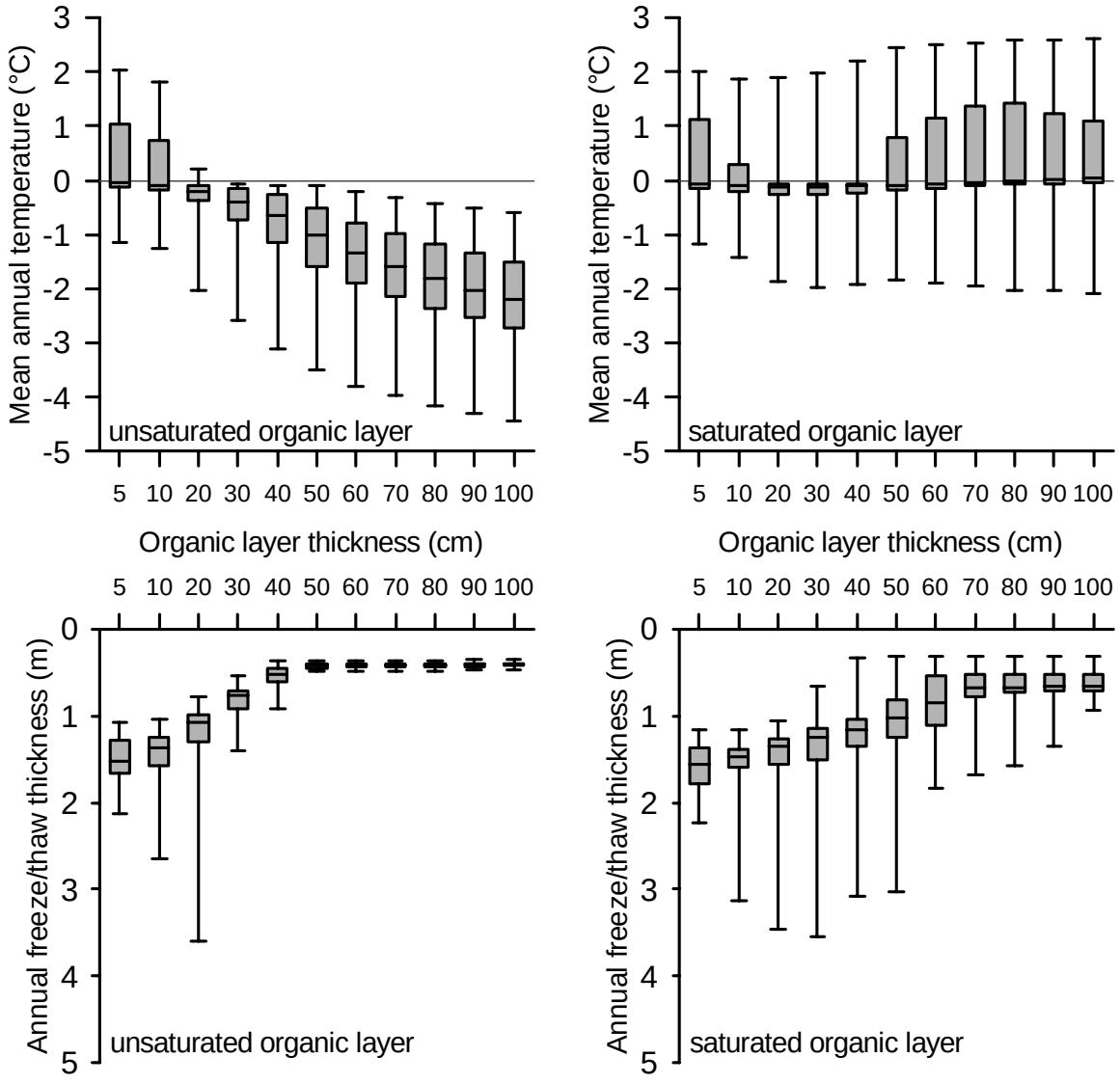

Figure 19. Effect of varying organic layer thickness on simulated mean annual temperature at the top-of-perennially frozen/unfrozen ground (TTOP) and maximum annual freezing/thawing layer thickness (AFTT) values for wet clay substrate terrain, using 1955-2006 Yellowknife climate statistics (preceded by 300-year spin-up). Boxes and whiskers show maximum, upper quartile, median, lower quartile and minimum values for 1955-2006 for each thickness.

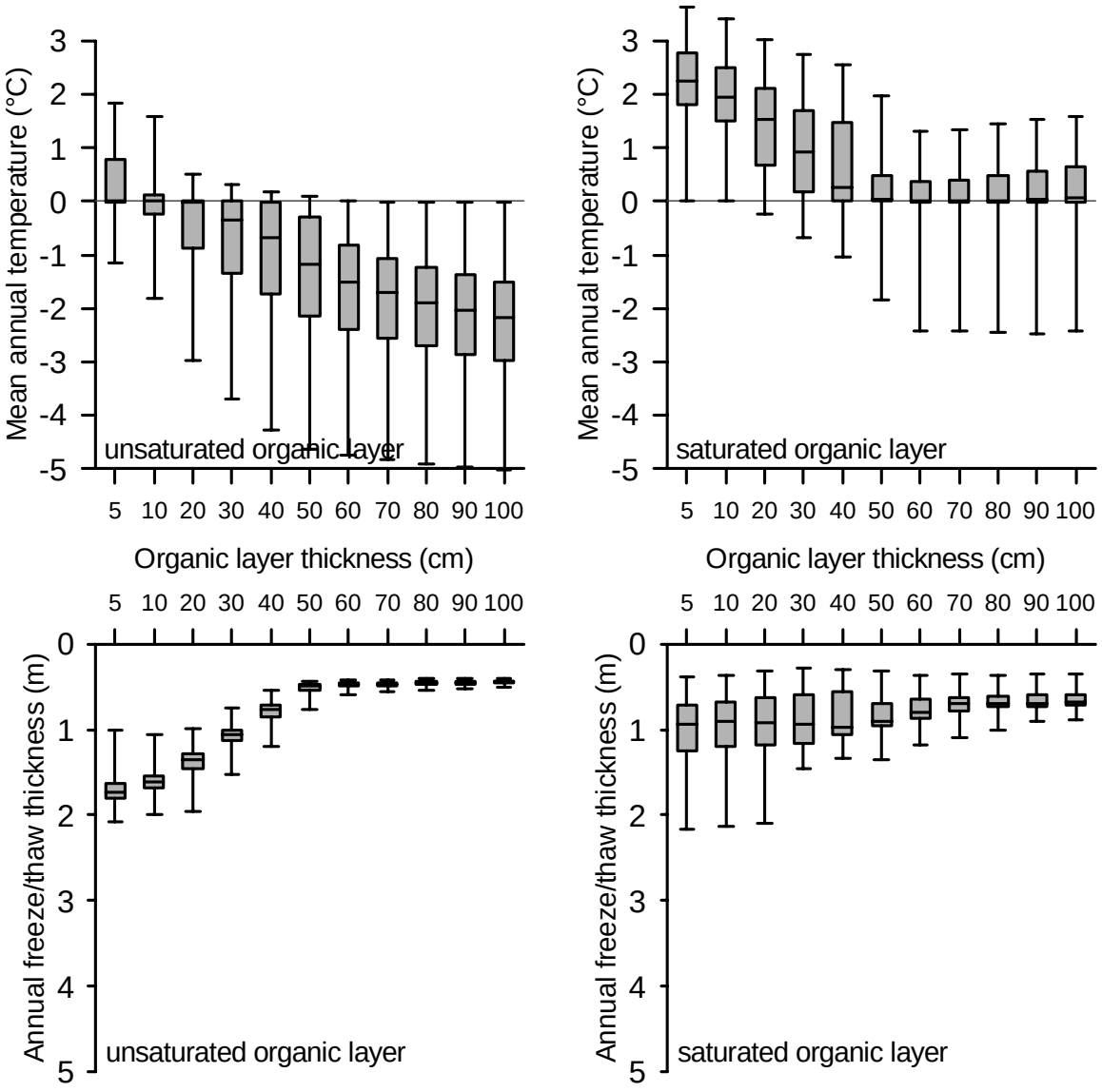

Figure 20. Effect of varying organic layer thickness on simulated mean annual temperature at the top-of-perennially frozen/unfrozen ground (TTOP) and maximum annual freezing/thawing layer thickness (AFTT) values for sand substrate terrain , using 1955-2006 Yellowknife climate statistics (preceded by 300-year spin-up). Boxes and whiskers show maximum, upper quartile, median, lower quartile and minimum values for 1955-2006 for each thickness.

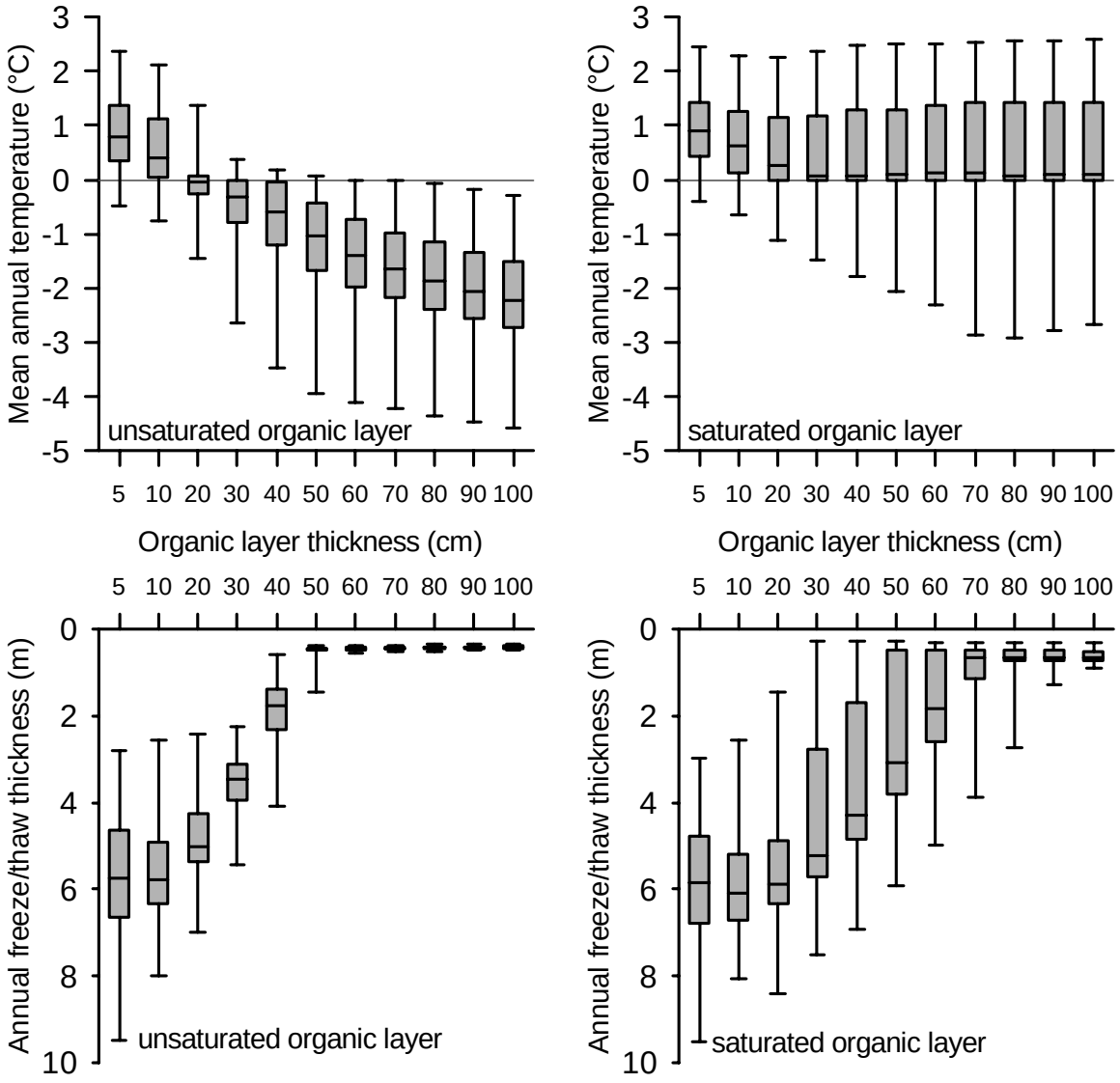

Figure 21. Effect of varying organic layer thickness on simulated mean annual temperature at the top-of-perennially frozen/unfrozen ground (TTOP) and maximum annual freezing/thawing layer thickness (AFTT) values for bedrock substrate terrain, using 1955-2006 Yellowknife climate statistics (preceded by 300-year spin-up). Boxes and whiskers show maximum, upper quartile, median, lower quartile and minimum values for 1955-2006 for each thickness.

Figure 22 combines mean results for all conditions and extends the simulated OLT range to 2 m. For cases with an unsaturated organic layer, AFTT and TTOP decrease as OLT increases. Mean AFTT in these cases reaches a minimum (about 60 cm) once the annual freezing/thawing layer is confined to the organic material. Mean simulated TTOP decreases rapidly as OLT increases to a depth of about 1 m (changing at a rate between 2 and 4°Cm^{-1}, below which the effect of increasing OLT is minimal (less than 0.2°Cm^{-1}).

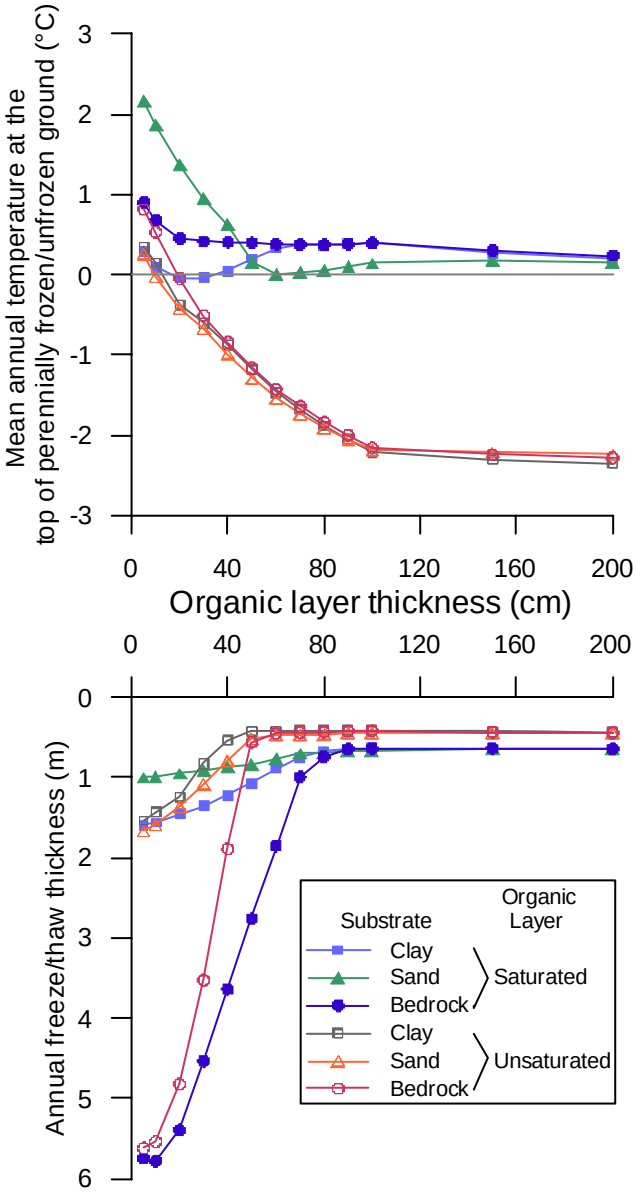

Figure 22. Effect of varying organic layer thickness on simulated mean annual temperature at the top-of-perennially frozen/unfrozen ground (TTOP) and average maximum annual freezing/thawing layer thickness (AFTT) values for wet clay, sand and bedrock substrate terrain, using 1955-2006 Yellowknife climate statistics (preceded by 300-year spin-up)

For cases with a saturated organic layer, mean AFTT shows a similar decrease as OLT increases, reaching a greater minimum depth (about 90 cm), while TTOP shows a complex relationship to OLT. While TTOP decreases continuously as OLT increases for the bedrock case, the sand and clay substrate cases both show a minimum TTOP at an intermediate OLT (30 cm for the clay substrate and 60 cm for the sand substrate). For the sand substrate case, mean simulated TTOP decreases rapidly as OLT increases to about 60 cm (about $4°Cm^{-1}$); for the bedrock and clay substrate cases, the decrease in TTOP (about $2°Cm^{-1}$) is less significant as OLT increases to about 30 cm. The temperature difference between the minimum (close to 0°C at 30-60 cm thickness) and with an OLT of 2 m is about 0.2 C° for the sand and clay cases.

Figure 23 shows the effect of organic layer moisture content on simulated TTOP and AFTT for a case with a wet clay substrate and a 1 m thick organic layer. Mean TTOP varies by 4°C over the entire range of moisture conditions, while mean AFTT varies within a relatively narrow range (about 50-65 cm). Mean TTOP is coldest with 20% saturation (porosity of 70-90%; volumetric moisture content of 14-18%), while mean AFTT is greatest with 30% saturation. Other than in the upper surface layers of an organic cover, moisture content this low is very unlikely in field conditions. At moisture contents greater than 30% saturation, TTOP increases by about 0.5°C for each 10 cm increment in OLT, while AFTT increases by about 2 cm for each increment.

DISCUSSION

Results of this study show that *any* difference in substrate materials produces a change in TTOP and AFTT. In approximate order of effect, the smallest differences (less than 0.1°C in TTOP and up to 13 cm in AFTT) were due to variations in the substrate well below the thickness of the annual freezing/thawing layer, and intermediate differences were due to differences in substrate materials within and immediately below the annual freezing/thawing layer itself. The greatest differences in TTOP were produced by changes in the thickness and degree of saturation of the surface organic layer.

Riseborough (2004) demonstrated that the insulating effect of the snow cover is influenced (in addition to the thickness and thermal properties of the snow itself) by the moisture content and thermal conductivity of the annual freezing/thawing layer. In organic soils, the combination of very low thermal conductivity at low water content and the very high water content at saturation (due to its high porosity) makes its thermal behaviour distinct from that of the mineral soils.

Recent studies (Throop *et al*., 2012, Karunaratne, 2011) have noted the strong dependence of freezing ground temperatures on the moisture content of the ground. The thickness of the organic surface layer determines the extent to which the moisture content of the organic layer controls the thermal regime: with a thin surface layer, the properties of the mineral substrate will have a greater influence on the thermal regime; when the surface organic layer is thicker than the AFTT, the properties of the mineral substrate will have little influence on the ground thermal regime, since most thermal offset effects are confined to the annual freezing/thawing layer.

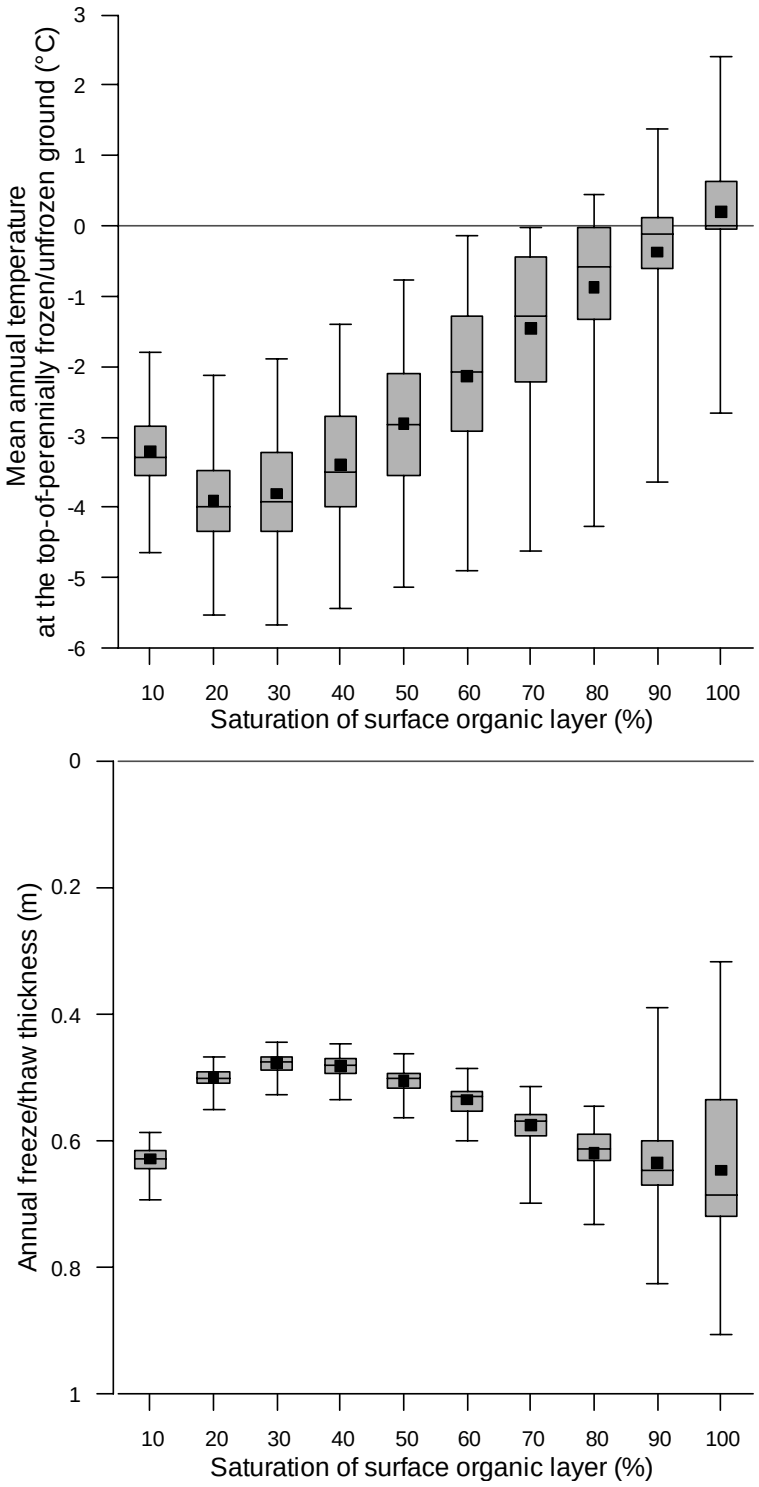

Figure 23. Effect of varying organic layer moisture content on simulated mean annual temperature at the top-of-perennially frozen/unfrozen ground (TTOP) and average maximum annual freezing/thawing layer thickness (AFTT) values for wet clay terrain, using 1955-2006 Yellowknife climate statistics (preceded by 300-year spin-up). Boxes and whiskers show maximum, upper quartile, median, lower quartile and minimum values for 1955-2006 for each degree of saturation

CONCLUSIONS

Of the conditions studied, modelling to correctly account for annual freezing and thawing degree-days, and a reasonably accurate representation of the average snow cover evolution (especially arrival, accumulation and density) are necessary to produce reasonably accurate model results.

Comparing thermal regimes of different substrates, the smallest differences in TTOP were due to variations in the substrate well below the thickness of the annual freezing/thawing layer, and intermediate differences were due to differences in substrate materials within and immediately below the annual freezing/thawing layer itself. The greatest differences in TTOP were produced by changes in the thickness and degree of saturation of the surface organic layer. Modelling results demonstrate the effect of variations in the properties of the organic surface layer on the thermal regime. Thickness variations from 0.1 to 1 m of organic soil produce variations of 2 to 3°C in mean annual ground temperature for the cases examined. Extreme variations in the moisture content of a 1 m thick organic layer produced a 5°C mean annual temperature range in simulation results; for the practical range of variation in saturation (40% – 100%) this variation is on the order of 3°C. These results suggest that of the thickness and moisture content of organic soil veneers are important determinants of permafrost conditions in this environment.

Confidence in the relative ordering of thermal regimes of different environments based on differences in substrate materials is high; however, field verification and further modelling are required to validate the actual predicted ground temperatures, and by extension the actual distribution of permafrost in the NGSR. In addition, local variations in snow cover regimes associated with topography and vegetation cover may produce thermal regime variations of equal magnitude to those due to the substrate.

Application to 1-D modelling

This analysis of the Yellowknife climate record provides a set of simple parameters for use in numerical modelling. Retaining accurate values for TDD_{Ann} and FDD_{Ann} is the most important aspect of the surface temperature climate. The results of the initial sensitivity analysis demonstrate the importance of correctly accounting for the seasonal evolution of the snow cover to the accuracy of the thermal results: the parabolic accumulation function was shown to represent the mean snow accumulation function for the Yellowknife record with the proper parameters, although the seasonal trend in snow density and the timing of the maximum snow depth within the season was identified as an additional parameter to be collected. Details of end-of-season snowpack evolution were shown to be of secondary importance. Based on the findings of the sensitivity analysis, further modification of the model allowing for the specification of the seasonal trend in snow density and the timing of the maximum snow depth in multi-year simulations is recommended.

Future work

The approach used for this phase was to match the snow accumulation function to the mean snow density to produce reasonably accurate results, due to the limited options for snow density variation provided in TONE. The accuracy of simulations in the next phase of this study could be improved by incorporating an empirical densification schemes such as in Verseghy (1991) to approximate the evolution of snow thermal properties over time.

The results of this study will be used to guide spatial and 2-d modelling in the NGSR. Two dimensional modelling will be used to evaluate some key landscape transitions, including lake and road edges and transitions between areas with a soil or peatland overburden and bedrock outcrop. In addition, 2-d modelling will be used to examine the special thermal conditions of hummocky

terrain. The fine-scale geometry and heterogeneity of hummocky terrain makes it difficult to characterize from field monitoring and difficult to model in one dimension (i.e. as a temperature profile). 2-D modelling of the thermal regime of a hummock field (including hummock geometry, with concomitant lateral variations in soil materials, soil moisture, and snow cover) will allow the appropriate specification of representative values for these thermal parameters in one-dimensional models, making it possible to scale up from local to regional spatial models.

ACKNOWLEDGEMENTS

This research was undertaken as part of the TRACS project, Geological Survey of Canada. The authors thank Dr. Yu Zhang of the Canada Centre for Remote Sensing for his useful comments.

REFERENCES

Arons, E. M. and Colbeck, S.C.. 1995. Geometry of heat and mass transfer in dry snow; a review of theory and experiment. *Reviews of Geophysics*. 33 (4): 463-493.

Aspler, L.B., 1978. Surficial geology, permafrost and related engineering problems: in Mineral Industry Report, 1976: Indian and Northern Affairs Canada, Geology Division, Yellowknife, Northwest Territories, EGS 1978-11, p. 119-135.

Bouchard C. 1990. Simulation du régime thermique des sols pergélisolés: essai du modèle TONE. Université Laval, Département de Géographie, Mémoire de Maîtrise, 137 p.

Brown, R.D., Brasnett B. & Robinson, D. 2003. Gridded North American Monthly Snow Depth and Snow Water Equivalent for GCM Evaluation. *Atmosphere-Ocean*, 41 (1): 1–14.

Brown, R.J.E. 1973. Influence of climatic and terrain factors on ground temperatures at three locations in the permafrost region of Canada. *Proceedings, Second International Conference on Permafrost, Yakutsk, USSR, North American Contribution*, pp. 27-34.

Burn, C.R. 1998. The active layer: two contrasting definitions. *Permafrost and Periglacial Processes*. vol. 9: pp. 411-416

Colbeck, S.C. 1991. The layered character of snow covers. *Reviews of Geophysics*, 29(1): 81-96.

EBA Engineering Consultants Limited, 1995. Yellowknife Highway (No. 3), N.W.T., km 242 to km 256, Preliminary Geotechnical Evaluation; Project 0701-95-11776, 14 p.

EBA Engineering Consultants Limited, 1998. Conceptual Road Design Study, N.W.T. HWY. No. 3., km 243.9 - km 256.4; Project 0701-98-13330, 13 p.

EBA Engineering Consultants Limited, 2003a. Yellowknife Highway (No. 3), Ground Temperature Cable Installation As-Built Report; Project 0701-95-1700051.506, 3 p.

EBA Engineering Consultants Limited, 2003b. Preliminary Geothermal Evaluation Yellowknife Highway (NWT No. 3), Km 252 + 680 & Km 262 +330; Project 0701-95-1700051.506, 12 p.

Ecosystem Classification Group. 2008. Ecological Regions of the Northwest Territories – Taiga Shield. Government of the Northwest Territories, Yellowknife, NT, Canada, viii + 149 p. + insert map.

Environment Canada, 2012. Canadian Climate Normals or Averages 1971-2000, http://climate.weatheroffice.gc.ca/climate_normals/index_e.html

Ferguson, R.I. 1999. Snowmelt runoff models. *Progress in Physical Geography*, 23: 205–227.

Gaandarse, A. 2011. Seasonal Thaw Depths in Relation to Surficial Characteristics in the Taiga Shield High Boreal Ecoregion Surrounding Yellowknife, Northwest Territories. Department of Geography, Carleton University, BA Thesis, 59 p.

Goodrich, L.E. 1982. The influence of snow cover on the ground thermal regime. *Canadian Geotechnical Journal*, 19: 421-432.

Groisman, P.Y. and T.D. Davies. 2001. Snow cover and the climate system. in *Snow Ecology.* J.G. Jones, J.W. Pomeroy, D.A. Walker and R.W. Hoham (Eds.). Cambridge University Press, New York, pp. 1-44.

Heginbottom, J.A., Dubeuil, M.A., and Harker, P.T. 1995. Canada, Permafrost. The National Atlas of Canada, 5th ed. Ottawa: Natural Resources Canada.

Hoeve, T.E., Seto, J.T.C., Hayley, D.W. 2004. Permafrost response following reconstruction of the Yellowknife Highway. *Proceedings of the International Symposium on Cold Regions Engineering, Vol.12, [Cold regions engineering and construction conference 2004, Edmonton, AB, Canada, May 16-19, 2004]* unpaginated.

Karunaratne, K.C., 2011. A Field Examination of Climate-Permafrost Relations in Continuous and Discontinuous Permafrost of the Slave Geological Province. Doctoral Dissertation, Carleton University , 281 pages.

Karunaratne, K.C., Kokelj, S.V., Burn, C.R. 2008. Near-surface permafrost conditions near Yellowknife, Northwest Territories, Canada. **in** D.L. Kane and K.M. Hinkel (eds.) Ninth international conference on Permafrost. International Conference on Permafrost (ICOP) Proceedings, Vol.9, p.907-912;

Kojima, K. 1967. Densification of seasonal snow cover. *Physics of Snow and Ice*, 2: 929–952, Institute of Low Temperature Science, Sapporo.

Lemmen, D.S., Duk-Rodkin, A. and Bednarski, J.M. 1994. Late glacial drainage systems along the northwestern margin of the Laurentide Ice Sheet. *Quaternary Science Reviews,* 13, p. 805-828.

Ling, F. & Zhang, T. 2006. Sensitivity of ground thermal regime and surface energy fluxes to tundra snow density in northern Alaska. *Cold Regions Science and Technology* 44: 121–130.

Ling, F. & Zhang, T. 2007. Modelled impacts of changes in tundra snow thickness on ground thermal regime and heat flow to the atmosphere in northernmost Alaska. *Global and Planetary Change* 57: 235-246.

Majorowicz, J. & Grasby, S.E. 2010. Heat flow, depth-temperature variations and stored thermal energy for enhanced geothermal systems in Canada. *Journal of Geophysics and Engineering* 7(3): 232-241.

Meteorological Service of Canada, 2000. Canadian Snow Data: Daily snow depth and snow water equivalent. (Digital media: CD-ROM) Climate processes and earth observation division, Downsview, Ontario, Canada.

Osokin, N.I., Samoylov, R.S., Sosnovskiy, A.V., Sokratov, S.A. & Zhidkov, V.A. 2000. Model of the influence of snow cover on soil freezing. *Annals of Glaciology*, 31: 417–421.

Pomeroy, J.W. 1998. An evaluation of snow accumulation and ablation processes for land surface modelling. *Hydrological Processes*. 12: 2339-2367.

Pomeroy, J.W. and E. Brun 2001. Physical Properties of snow. In Jones *et al*. (editors), *Snow ecology: an interdisciplinary examination of snow-covered ecosystems,* Cambridge University Press, *pp. 45-126*.

Pomeroy, J.W. and B.E. Goodison. 1997. Winter and snow. *in* **The surface climates of Canada**. W.G. Bailey, T.R. Oke and W.R. Rouse (Eds.). McGill-Queen's University Press, Montreal, pp. 68-100.

Riseborough, D.W. 2004. Exploring the parameters of a simple model of the permafrost-climate relationship. PhD Dissertation, Carleton University, Ottawa. 330 p.

Riseborough, D.W. 2007. The effect of transient conditions on an equilibrium permafrost-climate model. *Permafrost and Periglacial Processes* 18: 21–32.

Riseborough, D.W. and Smith, M.W. 1993. Modelling permafrost response to climate change and climate variability. *Proceedings, Fourth International Symposium on Thermal Engineering and Science for Cold Regions. Hanover, New Hampshire, U.S.A.*, pp. 179-187.

Riseborough D.W., Wolfe S., Duchesne, C, 2012. Simplified climate statistics for permafrost modeling: Yellowknife Case Study. *Proceedings of the Tenth international conference on permafrost; international contributions* (edited by K.M. Hinkel); The Northern Publisher, Salekhard, Yamal-Nenets Autonomous District, Russia, 2012 pp. 335-340.

Smith, D.G., 1994. Glacial lake McConnell: Paleogeography, age, duration, and associated river deltas, mackenzie river basin, western Canada. *Quaternary Science Reviews*, 13, p. 829-843.

Smith, M.W. and Riseborough, D.W. 1996. Ground temperature monitoring and detection of climate change. *Permafrost and Periglacial Processes*, 7: 301-310.

Smith, M.W., & Riseborough, D.W. 2002. Climate and the limits of permafrost: a zonal approach. *Permafrost and Periglacial Processes* 13: 1–15.

Smith, S.L., Wolfe, S., Riseborough, D. W. & Nixon F. M. 2009. Active-layer characteristics and summer climatic indices, Mackenzie Valley, Canada. *Permafrost and Periglacial Processes* 20: 201-220.

Sturm, M., Holmgren, J. and Liston, G.E.. 1995. Seasonal snow cover classification system for local to global applications. Journal of Climate. 8 (5): 1261-1283.

Sturm, M., Holmgren, J., König, M., Morris, K. 1997. The thermal conductivity of seasonal snow. *Journal of Glaciology* 97 (B2): 2129-2139.

Throop, J. , Lewkowicz, A.G. , Smith, S.L., 2012. Climate and ground temperature relations at sites across the continuous and discontinuous permafrost zones, northern Canada. *Canadian Journal of Earth Sciences*, 49: 865-876.

Van Everdingen, R.O. 1998. Multi-language glossary of permafrost and related ground-ice terms. International Permafrost Association. University of Calgary Printing Services. 268 p.

Verseghy, D. L. 1991. CLASS: A Canadian land surface scheme for GCMs I: Soil model. *International Journal of Climatology*, 11: 111–133.

Wolfe, S. A., Delaney, S., Duchesne, C., 2011. An inventory of borrow pits and pond development between 1961 to 2005, Highway 3, Yellowknife region, Northwest Territories. Geological Survey of Canada Open File 6948. 42 pages; 1 CD-ROM, doi:10.4095/289032

Wolfe, S.A. (Ed.) 1998. Living with Frozen Ground: a field guide to permafrost in Yellowknife, Northwest Territories. Geological Survey of Canada, Miscellaneous Report 64, 71 p.

Zhang, T., Osterkamp, T. E., & Stamnes, K. 1996. Influence of the depth hoar layer of the seasonal snow cover on the ground thermal regime, *Water Resources Research*, 32: 2075-2086.

Zhang, T.J., 2005. Influence of the seasonal snow cover on the ground thermal regime: an overview. *Reviews of Geophysics*, 43: RG4002.